Praca wykonana w ramach projektu TEAM kierowanego przez Prof. Pawła Moskala. Projekt finansowany przez Fundację na rzecz Nauki Polskiej.

This work is supported by the Foundation for Polish Science under Grant TEAM/2017-4/39

JAGIELLONIAN UNIVERSITY
FACULTY OF PHYSICS, ASTRONOMY
AND APPLIED COMPUTER SCIENCE
INSTITUTE OF PHYSICS

Mateusz Bała

Album number: 1078645

Polarization formalisms and quantum entanglement in the positronium systems

Master's Thesis in Physics

Thesis prepared in the Nuclear Physics Division
of the Jagiellonian University supervised by

dr Michał Silarski

Cracow, 2022

Abstract

Quantum entanglement of the group of particles, is a fascinating quantum mechanical phenomenon, without the classical analogy, which happens when the system state can be treated only as a whole, and the constituent particles cannot be described separately. The simplest example in which the quantum entanglement can be manifested is the polarized two-photon system. Indeed such a case was analyzed both theoretically and experimentally many times. However, most of the studies were concentrated on the optical photons regime. For higher-energetic photons, the polarization cannot be measured by using standard devices such as polarizers. However, the partial polarization estimation is possible by exploiting the Compton scatterings process. In this work, the analysis of a high-energetic, polarized two-photon system probed by the doubly Compton scattering process, is considered. The model is described using the quantum information theory formalism. In addition, the model is incorporated to the Monte Carlo C++ library. The simulations of the various quantum states are performed and the results are compared with the expectations from the theory.

Streszczenie (Abstract in Polish)

Splątanie kwantowe zespołu cząstek to fascynujące zjawisko mechaniki kwantowej, pozbawione klasycznej analogii, które ma miejsce, gdy stan układu można traktować tylko jako całość, a cząstek składowych nie da się opisać oddzielnie. Najprostszym przykładem, w którym może zamanifestować się splątanie kwantowe, jest spolaryzowany układ dwufotonowy. Układ ten był wielokrotnie analizowany zarówno teoretycznie, jak i eksperymentalnie. Jednak większość badań koncentrowała się na zakresie fotonów optycznych. W przypadku fotonów o wyższej energii polaryzacji nie można zmierzyć za pomocą standardowych urządzeń, takich jak polaryzatory. Jednak częściowe oszacowanie polaryzacji jest możliwe dzięki wykorzystaniu procesu rozpraszania Comptona. W niniejszej pracy rozważana jest analiza wysokoenergetycznego, spolaryzowanego układu dwufotonowego, próbkowanego w procesie podwójnego rozpraszania Comptona. Model zjawiska opisano przy użyciu formalizmu kwantowej teorii informacji. Opisany proces został zaimplementowany w postaci biblioteki Monte Carlo C++. Następnie, przeprowadzano symulacje różnych stanów kwantowych, a wyniki porównano z przewidywaniami teorii.

Contents

Chapter 1

Introduction

1.1 Introduction

Quantum mechanics (QM) is a fundamental theory describing the behaviour of particles in the atomic and the subatomic scale [12]. Many of the QM phenomena cannot be explained by the classical analogies, which on one hand makes QM difficult to interpret and understand, on the other hand makes it fascinating. Quantum entanglement (QE) is one of such a phenomena. QE of the group of particles appears, when the system state can be treated only as a whole, and the constituent particles cannot be described separately. The simplest example in which the QE can be manifested is the two-photon system.

The photon polarization is a degree of freedom, which is the quantum analog of the classical polarization of the electromagnetic wave interpreted as the geometrical orientation of the oscillation of the electric field with respect to the direction of propagation.

The polarization of the two-photon system was analyzed both theoretically and experimentally many times. Indeed, the canonical experiments and paradoxes of QM such as EPR were analysed in the two-photon systems [3]. However, most of the studies were concentrated on the optical photons regime, where the light polarization can be measured by using standard optical devices such as polarizers. For higher-energetic photons, the partial polarization estimation is still possible by exploiting the Compton scatterings process [19].

The measurement of the photon polarization with Compton scattering was recently proposed in the context of the development of novel medical imagining techniques in positron emission tomography by the J-PET project [18]. In the positron emission tomography the radio-pharmaceutical administered to the patient is absorbed by the patients cells. Further, the radio-isotopes decay via β^+ process and consequently the positron is emitted. Next, the positron together with an electron from the human body can

form a meta-stable atom called positronium. The positronium atom is likely to decay into a pair of two photons. The properties of such a system can be experimentally measured by using the J-PET detector [18], which apart from being the prototype medical scanner turn out to be a perfect device for the fundamental physics studies [18], including the investigation of the quantum photon correlations [18].

In the process of preparation to the experimental measurements as well as during the data analysis, it is of high importance to be able to compare the experimental data with the Monte Carlo simulations based on the theoretical models implementations.

There exist several physics simulation libraries such as Geant4 [1] that provide various implementations of Compton scattering for polarized and unpolarized photons, however their functionality is very limited. None of them support the concept of the correlated photons nor allow choosing the arbitrary initial polarization states.

In the frame of this thesis, the polarized two-photon system probed by the doubly Compton scattering process, is considered. The model is based on the quantum information theory formulation proposed by prof. Beatrix Hiesmayr [13]. The model is implemented in the form of the Monte Carlo library, that can be used to simulate a various experimental observables of the two-photon system originating from the decay of the positronium state.

1.2 Scope of the thesis

The objective of this thesis is the development of the Monte Carlo simulation model describing the two-photon correlation system probed by the doubly Compton scattering. The mathematical description of Compton scattering is given in the quantum information formulation in the language of Kraus operators. The model is incorporated to the Monte Carlo C++ library.
The simulations of the various quantum states are performed and the results are compared with the expectations from the theory.

The thesis is composed of 5 chapters. In the theoretical part, I provide the introduction to the concept of photon polarization state Sec.2.1, then I focus on the theory of the density probability matrices and I introduce the Kraus operators concept Sec.2.4. In the next chapter, short reminder of the Compton scattering process is given Sec.2.5. Next section Sec.2.6 is dedicated to the reformulation of the Compton process in the language of the Kraus operators. Final part Sec.2.7 of theory covers the concept of the observable for the J-PET [19] experiment and prediction of it shapes for different polarization states. The second part of the thesis presents the implementation Sec.3 of the Monte Carlo simulations and the results for the separated states Sec.4.1, mixed states Sec.4.2 and entangled states Sec.4.3. The thesis is summarized in the last chapter Sec.5.

The results presented in this thesis were obtained in the frame of the J-PET project, under the guidance of Dr. Wojciech Krzemien, with collaboration of prof. Beatrix Hiesmayr.

Chapter 2

Theory

2.1 Photon and polarization states

Historically, the beginning of the concept of photon has started [24] with the Einstein explanation of the photoelectric effect in 1905. He postulated that a light being an electromagnetic wave of the frequency ω and described by the wave vector $\vec{k}$ of length $k = \frac{\omega}{c}$ must, in some situations, be treated as quantized. Thus, Einstein suggested that the light in fact consists of particles with the energy $E = \hbar\omega$ and the momentum $\vec{p} = \hbar\vec{k}$,which received a name "photon" by the Gilbert Lewis in 1926 [24]. In today's modern particle theories [7]. photon is treated as massless particle with the intrinsic angular momentum (spin) equal to 1 . Furthermore, it is a carrier of the electromagnetic interactions and it obeys the Bose-Einstein statistics. Finally, even to a single photon we can attribute the property called polarization.

The photon polarization is a degree of freedom, which is the quantum analog of the classical polarization of the electromagnetic wave interpreted as the geometrical orientation of the oscillation of the electric field with respect to the direction of propagation.

There exists several formalisms to describe the polarization of light. Some of them are rooted in the classical wave-based description of light, therefore we will start with it.

As it was mentioned above, the light is an oscillation of the electromagnetic field. First, we should start from the classical interpretation [4], where the light vibration is defined by the vibrating vector, which can be introduced from the Maxwell's equations. The electric field $E(t)$ is real-valued however we introduce it is a complex field and its observable part is its real part. To do that we represent the real field as a Fourier integral:

$$E(t) = \int_{-\infty}^{\infty} d\omega e^{-i\omega t} E(\omega)$$

where $E(\omega)$ is the field spectral amplitude. Additionally, lets split this integral into two parts known as the positive-frequency and negative-frequency

fields [11]:

$$E^{(+)}(t) = \int_0^\infty d\omega e^{-i\omega t} E(\omega)$$

$$E^{(-)}(t) = \int_{-\infty}^0 d\omega e^{-i\omega t} E(\omega)$$

which are complex conjugates (because the spectral amplitude of real field $E^*(\omega) = E(-\omega)$):

$$[E^{(+)}(t)]^* = E^{(-)}(t),\ [E^{(-)}(t)]^* = E^{(+)}(t)$$

The observed field is proportional to its real part as mentioned before:

$$E(t) = E^{(+)}(t) + E^{(-)}(t) = \mathrm{Re}\{E^{(+)}(t)\}$$

Let's define the wave plane with two orthogonal unit vectors ($\hat{x}$,$\hat{y}$,$\hat{x} \cdot \hat{y} = 0$) on it and let $\hat{z}$ be the direction of wave propagation, hence the vibration of the electric field $\vec{E}$ is [11]:

$$\vec{E} = \mathrm{Re}\{(a\hat{x} + b\hat{y}e^{i\phi})e^{i(\omega t - kz - \Phi)}\} \tag{2.1}$$

$$E_x = a\cos(\omega t - kz - \Phi),\ E_y = b\cos(\omega t - kz - \Phi - \phi) \tag{2.2}$$

where Eq. 2.2 describes $\vec{E}$ components on the wave plane. For further discussion, we change the time of the wave origin in such way that:

$$E_x = a\cos(\omega t),\ E_y = b\cos(\omega t - \phi) \tag{2.3}$$

If the phase difference is $\phi = \frac{\pi}{2}$ we have left-handed elliptical polarization and for $\phi = \frac{-\pi}{2}$ we have right-handed elliptical polarization [11]. Additionally, if amplitudes $a = b$ we have analogous circular polarization. Moreover, for the phases $\phi = (2n+1)\pi$,$n \in \mathbb{Z}$ we have linear polarization (vibration vector oscillates along one line defined by the angle α by $b = a\cos\alpha$). Hence, any polarization can be always treated as the addition of two opposite circular polarizations.

In many cases we deal with the unpolarized light which is described by the same formula Eq. 2.3 however parameters a,b,ϕ are random functions of time [4] - in other words, the electric vector moves randomly, without preferred direction on the wave plane [11].

Presented results gives the most complete classical description of the polarization state of light in vector form. However, we can introduce two other representations of polarization, knows as the Jones and the Stokes representation.

2.1.1 Jones representation

Let's return the positive-frequency field and as we did it before, lets assume the plane wave propagates along the $\hat{z}$ [10]:

$$\vec{E}^{(+)}(r,t) = \vec{E}_0(t)e^{-i\omega t+ikz}$$

where $\vec{E}_0(t)$ is the amplitude which we decompose in two vectors along the $\hat{x}$ (horizontal,H) and the $\hat{y}$ (vertical,V) direction:

$$\vec{E}_0(t) = \vec{E}_H(t) + \vec{E}_V(t)$$

The Jones vector is defined as [10],[22]:

$$\vec{\epsilon} = \begin{pmatrix}\alpha\\ \beta\end{pmatrix} = \frac{1}{\sqrt{S_0(t)}}\begin{pmatrix}E_H(t)\\ E_V(t)\end{pmatrix}$$

where $S_0(t)$ is the instantaneous intensity of the light wave:

$$S_0(t) = |E_H(t)|^2+|E_V(t)|^2 \tag{2.4}$$

Parameters α and β meet the normalization condition $|\alpha|^2+|\beta|^2= 1$ and we define them as:

$$\alpha = \cos\frac{\vartheta}{2},\ \beta = e^{i\phi}\sin\frac{\vartheta}{2}$$

where $\vartheta \in [0,\pi]$ and $\phi \in [0,2\pi)$ is the relative phase. For such defined Jones vector we can define linear polarized light ($\phi = 0$) [10]:

$$\vec{\epsilon}_H = \begin{pmatrix}1\\ 0\end{pmatrix},\ \vec{\epsilon}_V = \begin{pmatrix}0\\ 1\end{pmatrix}$$

or diagonal ($\alpha = \beta = \frac{1}{\sqrt{2}}$) and anti-diagonal ($\alpha = -\beta = \frac{1}{\sqrt{2}}$) polarization [10]:

$$\vec{\epsilon}_D = \frac{1}{\sqrt{2}}\begin{pmatrix}1\\ 1\end{pmatrix},\ \vec{\epsilon}_A = \frac{1}{\sqrt{2}}\begin{pmatrix}1\\ -1\end{pmatrix}$$

or if change in the definition of D/A the phase from $\phi = 0$ to $\phi = \frac{\pi}{2}$ we receive the right-/left-circularly polarization [10]:

$$\vec{\epsilon}_R = \frac{1}{\sqrt{2}}\begin{pmatrix}1\\ i\end{pmatrix},\ \vec{\epsilon}_L = \frac{1}{\sqrt{2}}\begin{pmatrix}1\\ -i\end{pmatrix}$$

2.1.2 Stokes representation

The Jones vector is directly related to the electric field [22], therefore it is not suitable for representing the partially polarized or unpolarized light. The Stokes vectors were introduced to mitigate this problem [22]:

$$\vec{S} = \begin{pmatrix}S_1\\ S_2\\ S_3\end{pmatrix} \tag{2.5}$$

$$S_1 = |E_H|^2 - |E_V|^2 \tag{2.6}$$

$$S_2 = 2\mathrm{Re}\{E_H^* E_V\} \tag{2.7}$$

$$S_3 = 2\mathrm{Im}\{E_H^* E_V\} \tag{2.8}$$

$$S_0^2 = S_1^2 + S_2^2 + S_3^2 \tag{2.9}$$

where S_i are Stokes observables and S_0 is defined by Eq. 2.4 and the Eq. 2.9 describes the dependence between these observables. Furthermore, we can express observables S_2, S_3 in the same way as it is for S_1 but for different bases:

$$S_2 = |E_D|^2 - |E_A|^2$$

$$S_2 = |E_L|^2 - |E_R|^2$$

Hence, the Stokes observables can be interpreted as the difference of intensities measured in two orthogonal polarization modes [22]:

$$S_1 = I_H - I_V,\ S_2 = I_D - I_A,\ S_3 = I_L - I_R$$

The mean value $\bar{S}_j$ of the Stokes observables are called the Stokes parameters and we use them to describe the partially polarized light by the degree of polarization [10],[22]:

$$P = \sqrt{\sum_{j=1}^{3} \left(\frac{\bar{S}_j}{\bar{S}_0}\right)^2}$$

and the fully polarized light has $P = 1$, from the other side the unpolarized light has $P = 0$ and partially polarized light has this value between these two extremes. If we define the normalized Stokes vector we recover the connection with the Jones vector [22]:

$$\vec{\sigma} = \frac{\vec{S}}{S_0} = \begin{pmatrix} |\alpha|^2 - |\beta|^2 \\ 2\mathrm{Re}\{\alpha^*\beta\} \\ 2\mathrm{Im}\{\alpha^*\beta\} \end{pmatrix} = \begin{pmatrix} \cos\vartheta \\ \sin\vartheta\cos\phi \\ \sin\vartheta\sin\phi \end{pmatrix}$$

2.1.3 Quantum mechanic representation

We start this section from the particle state representation for the photon polarisation. First step is to define the space of polarization states which is the the Hilbert space $\mathcal{H}$ - the vector space over a complex $\mathbb{C}$ numbers with defined the complete scalar product [7]. For our purpose we define two-dimensional Hilbert space with the complete orthonormal basis $\{|H\rangle, |V\rangle\} \in \mathcal{H}$ ($\langle H|V\rangle = 0$,$\langle H|H\rangle = \langle V|V\rangle = 1$) and each element of this space (polarization state) can be expressed as:

$$|\vec{\epsilon}\rangle = \alpha\,|H\rangle + \beta\,|V\rangle \tag{2.10}$$

which is properly normalized $|\alpha|^2 + |\beta|^2 = 1$, $\alpha, \beta \in \mathbb{C}$. Here, we can treat the states $\{|H\rangle, |V\rangle\}$ as two eigenstates of the Pauli matrix σ_z:

$$\sigma_z = \begin{pmatrix} 1 & 0 \\ 0 & -1 \end{pmatrix},\ \sigma_z |H\rangle = |H\rangle,\ \sigma_z |V\rangle = -|V\rangle$$

However, definition of polarization state Eq. 2.10 includes the global phase which we cannot measure - it is possible to measure the difference between the states $\{|H\rangle, |V\rangle\}$. Due to that, we can replace above two complex numbers with three real numbers $\alpha, \beta, \phi \in \mathbb{R}$ where the last one is the relative phase between $\{|H\rangle, |V\rangle\}$:

$$|\vec{\epsilon}\rangle = \alpha |H\rangle + \exp(i\phi)\beta |V\rangle$$

We can parameterize α, β with an angle $\theta \in \mathbb{R}$ to automatically fulfil the normalization condition:

$$|\vec{\epsilon}\rangle = \cos\frac{\theta}{2} |H\rangle + \exp(i\phi) \sin\frac{\theta}{2} |V\rangle \tag{2.11}$$

The basis $\{|H\rangle, |V\rangle\}$ is not the only one - in fact we have an infinite number of possible basis choice. However, two other special bases are essential from the point of view of optics and the issues discussed in this work:

$$|D\rangle = \frac{1}{\sqrt{2}}(|H\rangle + |V\rangle),\ \ |A\rangle = \frac{1}{\sqrt{2}}(|H\rangle - |V\rangle) \tag{2.12}$$

$$|R\rangle = \frac{1}{\sqrt{2}}(|H\rangle + i|V\rangle),\ \ |L\rangle = \frac{1}{\sqrt{2}}(|H\rangle - i|V\rangle) \tag{2.13}$$

where Eq. 2.12 are two eigenstates of the Pauli matrix σ_x (linear polarization: diagonal and antidiagonal) and Eq. 2.13 are two eigenstates of the Pauli matrix σ_y (circular polarization: right- and left-hand):

$$\sigma_x = \begin{pmatrix} 0 & 1 \\ 1 & 0 \end{pmatrix},\ \sigma_x |D\rangle = |D\rangle,\ \sigma_x |A\rangle = -|A\rangle$$

$$\sigma_y = \begin{pmatrix} 0 & -i \\ i & 0 \end{pmatrix},\ \sigma_y |R\rangle = |R\rangle,\ \sigma_y |L\rangle = -|L\rangle$$

Now, we can define the Stokes and Jones vector for such states. To do that, first we have to use the occupation number representation defined in the Fock space - the infinite direct sum of set of Hilbert spaces $\mathcal{H}$ representing states with 0,1,...,N particles [8]:

$$\mathcal{F}(\mathcal{H}) = \bigoplus_{n=0}^{\infty} \mathcal{H}_n$$

where $\mathcal{H}_n$ is the Hilbert space with n-photons. Here, we will no focus on the detailed description [8] of the Fock space but instead we will use it do describe how to translate classical model of polarisation to the quantum one. To introduce that, first we have to replace the electric field with electric field operators and photon creation-annihilation operators. Such set of operators act on the quantum states of polarized light.

Here we consider a single mode specified by a plane-wave monochromatic modes. We have a quantization box with size L and we assume that the field distribution is periodic in all three Cartesian coordinates - only a discrete set of wave-vectors are allowed [15]:

$$\vec{k} = (k_x, k_y, k_z, \sigma),\ k_i = \frac{2n_i\pi}{L},\ n_i \in \mathbb{Z}$$

and σ is the polarization that can take one of two values (linear, circular, elliptic) - but these two polarization states have to be orthogonal. For such defined modes, we can define the quantum field as a superposition over modes [15]:

$$\hat{E}^{(+)}(\vec{r}, t) = \sum_k \hat{E}^{(+)} e^{i\vec{k}\vec{r} - \omega_{\vec{k}} t}$$

$$\hat{E}^{(-)}(\vec{r}, t) = \sum_k \hat{E}^{(-)} e^{i\vec{k}\vec{r} - \omega_{\vec{k}} t}$$

amplitudes $\hat{E}^{(+)}$, $\hat{E}^{(-)}$ are given as:

$$\hat{E}^{(+)} = c_{\vec{k}} a_{\vec{k}}$$

$$\hat{E}^{(-)} = c^*_{\vec{k}} a^\dagger_{\vec{k}}$$

where $a_{\vec{k}}$, $a^\dagger_{\vec{k}}$ are photon annihilation and creation operator in mode $\vec{k}$ (summation over the indices n_i) with frequency $\omega_{\vec{k}}$ and [17]:

$$c_{\vec{k}} = i\sqrt{\frac{\hbar\omega_{\vec{k}}}{2\epsilon_0 L^3}}$$

The Hamiltonian for each mode is given by [17]:

$$H_{\vec{k}} = \hbar\omega_{\vec{k}} \left(a^\dagger_{\vec{k}} a_{\vec{k}} + \frac{1}{2} \right)$$

For our further discussion lets use the linear polarization modes (H,V) defined by the not Hermitian operators $a^\dagger_{H,V} \neq a_{H,V}$ with the following not commutation and commutation relations:

$$[a_H, a^\dagger_H] = [a_V, a^\dagger_V] = 1$$

$$[a_H, a_V^\dagger] = [a_H, a_V] = ... = 0$$

which is strictly an effect of polarization modes orthogonality.

The annihilation (and creation) operators for different modes such as diagonal/antidiagonal (D,A) and righ-/left-circular (R,L) polarization modes are connected with horizontal/vertical modes via:

$$a_{D,A} = \frac{1}{\sqrt{2}}(a_H \pm a_V) \tag{2.14}$$

$$a_{R,L} = \frac{1}{\sqrt{2}}(a_H \pm i a_V) \tag{2.15}$$

Fort each mode the creation-annihilation operators form the photon-number $\hat{N}$ operators:

$$a_H^\dagger a_H = \hat{N}_H,\ a_V^\dagger a_V = \hat{N}_V$$

which are Hermitian ($\hat{N}_i^\dagger = \hat{N}_i$) and because of their Hermicity their corresponds to the real observables - they can be measured. The eigenvalues of this operators are non-negative integer numbers and are called the Fock states $|N\rangle$ - the number of photons populating a mode is fixed and does not fluctuate:

$$\hat{N}_i |N\rangle_i = N_i |N\rangle_i$$

and the annihilation-creation operators act on such states as follow:

$$a_j |N\rangle_j = \sqrt{N} |N-1\rangle_j$$

$$a_j^\dagger |N\rangle_j = \sqrt{N+1} |N+1\rangle_j$$

With such defined tools we can consider a single-photon state which is a superposition of N=1 Fock states in the horizontal and vertical polarization modes:

$$|\epsilon\rangle = \alpha |1\rangle_H |0\rangle_V + \beta |0\rangle_H |1\rangle_V = \alpha |1\rangle_H + \beta |1\rangle_V \tag{2.16}$$

where $|\alpha|^2+|\beta|^2= 1$. Let's comments what above equation means. As we said, the state of the single photon is a superposition of Fock space for N=1 (because one photon) which means we have two modes (H,V) and only one particle to occupy modes - hence we can have one photon in mode H and zero photons in mode V ($|1\rangle_H |0\rangle_V$) or zero photons in mode H and one photon in mode V ($|0\rangle_H |1\rangle_V$). Second part means that the photon spreads over two polarization modes H and V.

Moreover, from the Eq. 2.14 and Eq. 2.15 we have:

$$|1\rangle_D = \frac{1}{\sqrt{2}}(|1\rangle_H + |1\rangle_V),\ \ |1\rangle_A = \frac{1}{\sqrt{2}}(|1\rangle_H - |1\rangle_V)$$

$$|1\rangle_L = \frac{1}{\sqrt{2}}(|1\rangle_H + i\,|1\rangle_V),\ \ |1\rangle_R = \frac{1}{\sqrt{2}}(|1\rangle_H - i\,|1\rangle_V)$$

The Jones vector for one-photon state Eq. 2.16 is [5] [6]:

$$|\epsilon\rangle = \begin{pmatrix} \alpha \\ \beta \end{pmatrix}$$

We replace the classical Stokes observables with the Hermitian Stokes operators [5],[6]:

$$\hat{S}_0 = a_H^\dagger a_H + a_V^\dagger a_V$$
$$\hat{S}_1 = a_H^\dagger a_H - a_V^\dagger a_V$$
$$\hat{S}_2 = a_H^\dagger a_V + a_V^\dagger a_H$$
$$\hat{S}_3 = i(a_H^\dagger a_V - a_V^\dagger a_H)$$

which correspond to the real observables and have the following commutation relations:

$$[\hat{S}_0, \hat{S}_k] = 0, \ k \in 1, 2, 3 \tag{2.17}$$

$$[\hat{S}_k, \hat{S}_l] = i\epsilon_{klm}\hat{S}_m, \ k, l, m \in 1, 2, 3 \tag{2.18}$$

The equality Eq. 2.17 tells us that the polarization and the intensity are separated concepts - the form of polarization does not depend on it size (intensity). From the other hand, due to the noncommuation between operators in Eq. 2.18 we cant have the full information about the photon polarization because the measurement of one parameters has an impact on the other one.

The degree of the polarisation is defined as:

$$P = \sqrt{\sum_{j=1}^{3} \left(\frac{\left\langle \hat{S}_i \right\rangle}{\left\langle \hat{S}_0 \right\rangle} \right)^2}$$

2.1.4 Comparison of representations

The presented introduction of the concept of light polarization and its various representations in terms of classical and quantum physics shows a wide spectrum of possibilities for interpreting and measuring this property of light. For the full polarized light we can use the Jones representation which is directly related to the photon's electric field. From the other side, an alternative for partially polarized light it is better to use the Stokes representation. Both representations have their important roles in the classical optics and its quantum version can be applied to the quantum optics. For the purposes of this thesis, a natural approach dictates to use the Jones representation, however, due to the common use of the Stokes representation in programming libraries such as Geant4, it is important to present and understand it. In the table Tab. 2.1 a set of different representations is presented.

Table 2.1: Comparison of the polarisation representations

Type	Name	Jones $(\alpha, \beta)^T$	Stokes $(\sigma_1, \sigma_2, \sigma_3)^T$	QM state
linear	horizontal	$(1, 0)$	$(1, 0, 0)$	$\|H\rangle$
linear	vertical	$(0, 1)$	$(-1, 0, 0)$	$\|V\rangle$
linear	diagonal	$\frac{1}{\sqrt{2}}(1, 1)$	$(0, 1, 0)$	$\|D\rangle$
linear	antidiagonal	$\frac{1}{\sqrt{2}}(1, -1)$	$(0, -1, 0)$	$\|A\rangle$
circular	right-hand	$\frac{1}{\sqrt{2}}(1, i)$	$(0, 0, 1)$	$\|R\rangle$
circular	left-hand	$\frac{1}{\sqrt{2}}(1, -i)$	$(0, 0, -1)$	$\|L\rangle$

2.2 Two-photon state

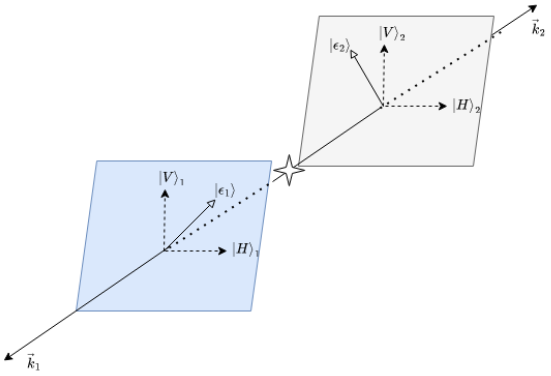

Figure 2.1: Two photons system. The star represents the emission point. Colored parallelogram represent the polarization plain for each photon.

Let's consider a most general polarized two-photon state described in the basis $\{|H\rangle_i, |V\rangle_i\},\ i \in \{1, 2\}$,

$$\begin{aligned} |\psi\rangle &= a\,|H\rangle_1\,|H\rangle_2 + b\,|H\rangle_1\,|V\rangle_2 + c\,|V\rangle_1\,|H\rangle_2 + d\,|V\rangle_1\,|V\rangle_2 \\ &= a\,|HH\rangle + b\,|HV\rangle + c\,|VH\rangle + d\,|VV\rangle \end{aligned} \tag{2.19}$$

where $a, b, c, d \in \mathbb{C}$ and $|a|^2 + |b|^2 + |c|^2 + |d|^2 = 1$. We can distinguish two types of states $|\psi\rangle$: separable and entangled. We say that the state $|\psi\rangle$ is separable if and only if it can be written as a tensor product of two one-photon states $|\psi\rangle = |\psi_1\rangle \otimes |\psi_2\rangle$, where $|\psi_i\rangle \in \mathbb{C}^2$. Otherwise a given state $|\psi\rangle$ is entangled.
For the state $|\psi\rangle$ we can derive a simple rule which distinguishes between separable and entangled states. Let's assume $|\psi\rangle = |\psi_1\rangle \otimes |\psi_2\rangle$ and $|\psi_1\rangle = \begin{pmatrix} x \\ y \end{pmatrix}$ and $|\psi_2\rangle = \begin{pmatrix} u \\ v \end{pmatrix}$ then we have that:

$$|\psi_1\rangle \otimes |\psi_2\rangle = \begin{pmatrix} xu \\ xv \\ yu \\ yv \end{pmatrix}$$

which implies that if $|\psi\rangle$ is separable then

$$\begin{pmatrix} a \\ b \\ c \\ d \end{pmatrix} = \begin{pmatrix} xu \\ xv \\ yu \\ yv \end{pmatrix}$$

and after simple algebraic calculations we obtain the separability condition for $|\psi\rangle$ as:

$$ad - bc = 0 \tag{2.20}$$

We can define as many entangled states as we want , for example the state below is an entangled one:

$$\frac{1}{\sqrt{2}}(|HV\rangle + e^{i\phi}|VH\rangle),\ \phi \in \mathbb{R},\ ad - bc = -e^{i\phi} \neq 0$$

however, there exist a preferred set of entangled states which create an orthonormal basis and plays an important role in the development of the quantum computing. The mentioned set of states is called the Bell states and it is defined as follows:

$$\left|\phi^{\pm}\right\rangle = \frac{1}{\sqrt{2}}(|HH\rangle \pm |VV\rangle),\ \left|\psi^{\pm}\right\rangle = \frac{1}{\sqrt{2}}(|HV\rangle \pm |VH\rangle)$$

We may ask which states there are more in terms of the two-photon system - separable or entangled? To answer that question first we have to come back to the idea of the Bloch sphere Fig. 2.2 which is the geometrical representation of a single quantum state (i.e. single photon polarisation). On the poles of such sphere we place the basis's vectors and require from the state to be normalized - explicitly, we postulate that our state is given by then Eq. 2.11. The Bloch sphere is 2-sphere S^2 ($\dim(S^2) = 3$), hence the space of 2-states like Eq. 2.19 is defined by the product of two Bloch spheres $S^2 \times S^2$ ($\dim(S^2 \times S^2) = \dim(S^2) + \dim(S^2) = 6$). All entangled states have to be in such 6-dimensional space, however the separable states lays in the subspace due to condition Eq. 2.20 - we have two dependent parameters which reduce the dimension of our space of states to the 4-dimensional subspace. From above, we see that the number of possible separable states is always less then the number of the entangled ones.

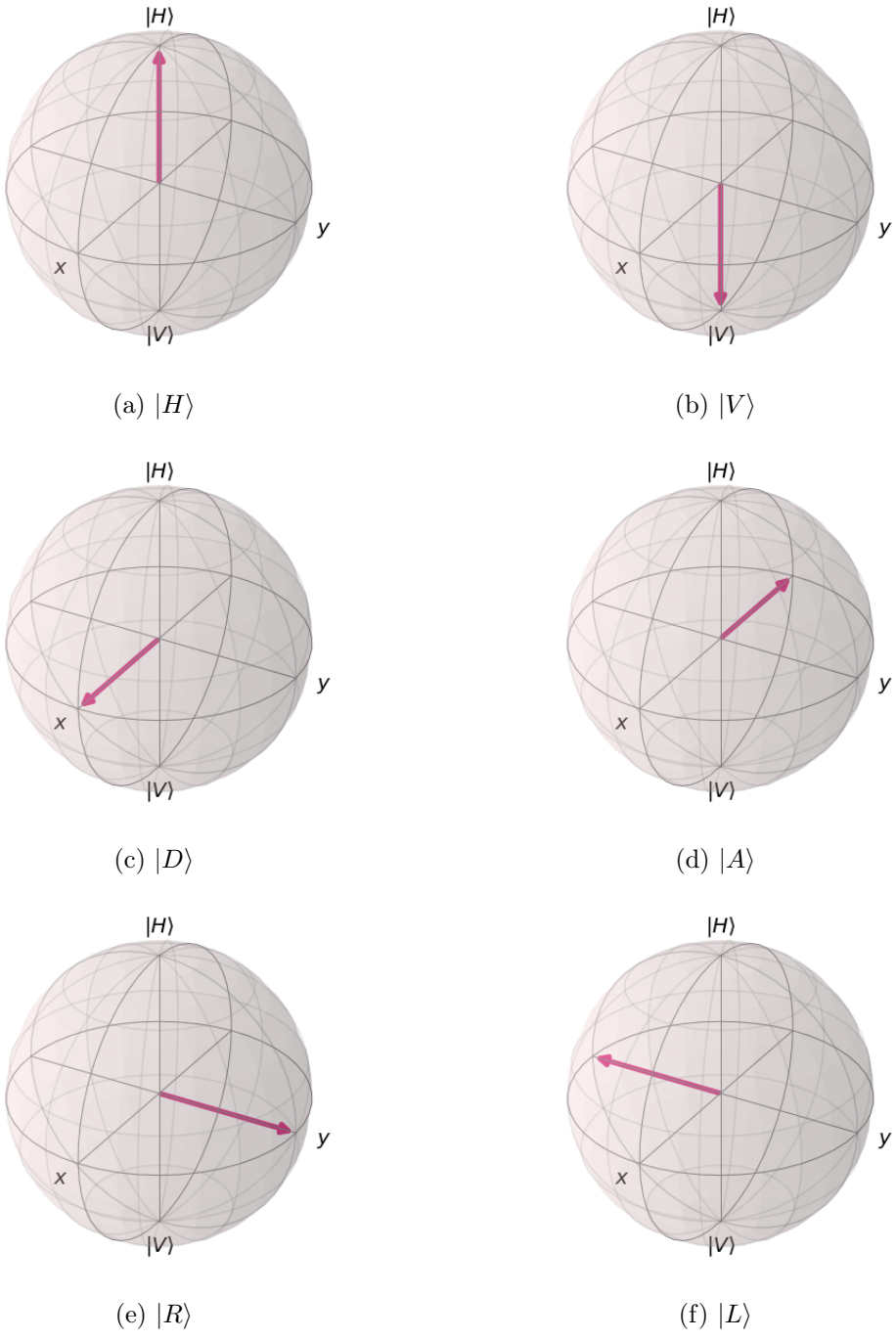

(a) $|H\rangle$ (b) $|V\rangle$

(c) $|D\rangle$ (d) $|A\rangle$

(e) $|R\rangle$ (f) $|L\rangle$

Figure 2.2: Visualization of the polarization bases on the Bloch sphere.

2.3 Mixed states and density operators

The state vector formalism allows to describe the photon systems corresponding to fully polarized (or coherent) light. However, if we want to be able to describe also a partly polarized light, we must use the density operator approach. This formalism is a generalization of the state-vector description.

If the photon system is fully polarized, then we say that the system is in the pure state, otherwise it is in the mixed state.

The mixed state captures the idea of the statistical mixture e.g. let's consider a source of light that produces the different polarization states (ensemble of the pure states $|\psi_1\rangle, ..., |\psi_n\rangle$) with different probabilities p_i such that $\sum_i p_i = 1$. The final system is described by so called density operator ρ defined as:

$$\hat{\rho} = \sum_k p_k |\psi_k\rangle \langle\psi_k|$$

The density operator is the Hermitian operator $\hat{\rho} = \hat{\rho}^\dagger$ with the unit trace $\mathrm{Tr}(\hat{\rho}) = 1$ and is non-negative $\forall |\phi\rangle \in \mathcal{H}\ \langle\phi| \hat{\rho} |\phi\rangle \geq 0$.

By given orthonormal basis $\{|i\rangle\}$ in n dimensional Hilbert space associated with the system we can define the corresponding matrix with density operator, known as the density matrix ρ_{ij}:

$$\rho_{ij} = \langle i| \hat{\rho} |j\rangle$$

. If we expand a pure state $|\psi_k\rangle$ over an orthonormal basis $\{|i\rangle\}$:

$$|\psi_k\rangle = \sum_i c_i^{(k)} |i\rangle, \ c_i \in \mathbb{C}$$

then the density matrix can be expressed as:

$$\begin{aligned} \rho_{ij} &= \sum_k p_k \langle i|\psi_k\rangle \langle\psi_k|j\rangle \\ &= \sum_k p_k c_i^{(k)} c_j^{(k)*} \end{aligned} \tag{2.21}$$

Now we can easily distinguish the mixed state from the pure one just by using a following rule:

$$\mathrm{Tr}(\hat{\rho}^2) \begin{cases} = 1, \text{pure state} \\ < 1, \text{mixed state} \end{cases}$$

The diagonal terms ρ_{ii} represents the probability P_i that the system is left in the state $|i\rangle$ after measuring the observable whose eigenstates are $\{|i\rangle\}$ (ρ_{ii} represents the population of the state $|i\rangle$):

$$\rho_{ii} = \mathrm{Tr}(\hat{\rho} P_i), \ P_i = |i\rangle \langle i|$$

The off-diagonal terms ρ_{ij} represents interference between the states $|i\rangle$ and $|j\rangle$ (we call ρ_{ij} as coherences). If $\rho_{ij} \neq 0$ even after averaging over the statistical mixture, q quantum-coherence effect between the states $|i\rangle$ and $|j\rangle$ remains.

Any mixed state density matrix can be expressed as a weighted sum of other density matrices, in an infinite number of different ways. From the other side, the pure state can only be expressed in one unique way.

2.4 System evolution

2.4.1 Unitary operation

To describe the evolution of a quantum system over time that is not disturbed by the external environment (closed system) we use the the unitary operation $U_t : \mathcal{H}_n \to \mathcal{H}_n$ which has to meet four conditions [14]:

$$\forall t \in \mathbb{R} \forall |\psi\rangle \in \mathcal{H}_n \ : \ \langle \psi U_t | U_t \psi \rangle = \langle \psi | \psi \rangle \tag{2.22}$$

$$\forall t \in \mathbb{R} \ : \ U_t \left(\sum_{i=1}^{n} \alpha_i |\psi\rangle \right) = \sum_{i=1}^{n} \alpha_i U_t |\psi\rangle \tag{2.23}$$

$$\forall t_1, t_2 \in \mathbb{R} \ : \ U_{t_1+t_2} = U_{t_1} \cdot U_{t_2} \tag{2.24}$$

$$\forall t_0 \in \mathbb{R} \ : \ \lim_{t \to t_0} U_t |\psi(0)\rangle = \lim_{t \to t_0} |\psi(t)\rangle = |\psi(t_0)\rangle \tag{2.25}$$

where Eq. 2.22 is th condition of keeping the norm (if at the beginning we have a probability distribution, then after the realization of evolution there is also a probability distribution), Eq. 2.23 requires from U_t that it transforms each of the base states of the $|\psi\rangle$ state independently, Eq. 2.25 tells us that the time evolution is continuous.

The function U_t satisfying the conditions Eq. 2.22,Eq. 2.23,Eq. 2.24 is represented by a group of unitary operators [14].

Additionally, if the U_t satisfying all four conditions we have the Stone's theorem telling us that there exists exactly one hermitian operator H satisfying the relation [14]:

$$U_t = \exp(-itH)$$

which gives us the evolution of the state:

$$|\psi(t)\rangle = \exp(-itH) |\psi(0)\rangle$$

If we differentiate the last equation we receive the Schrodinger's equation:

$$i \frac{d}{dt} |\psi(t)\rangle = H |\psi(t)\rangle$$

In the language of density matrix ρ we introduce the time evolution as:

$$U(\rho) = \sum_i p_i U |\psi_i\rangle \langle \psi_i| U^\dagger = U \rho U^\dagger$$

2.4.2 Measurement operation

Quantum measurement is described by the set of $\{M_i\}$ operators [20] operating in the state space of the measured system and we use them to calculate the probability distribution of possible results and to describe the state after

the measurement. Before the measurement, the probability that the measurement operation will give us i-th result is:

$$p(i) = \langle\psi|M_i^\dagger M_i|\psi\rangle$$

and the state of system after the measurement is:

$$|\psi'\rangle = \frac{M_i|\psi\rangle}{\sqrt{\langle\psi|M_i^\dagger M_i|\psi\rangle}}$$

The measurement operators meet the completness condition:

$$\sum_i M_i^\dagger M_i = \mathbb{1}$$

which make sure that the sum or all probabilities sum to the one.

In the language of the density matrices, the probability to measure the m-th value by the observable M_m for the state $|\psi_i\rangle$ is [20]:

$$p_{m|i} = \langle\psi_i|M_m^\dagger M_m|\psi_i\rangle = \mathrm{Tr}(M_m^\dagger M_m|\psi_i\rangle\langle\psi_i|)$$

and for the set of the initial states the probability to receive the value m-th is:

$$p_m = \sum_i p_{m|i}p_i = \sum_i p_i \mathrm{Tr}(M_m^\dagger M_m|\psi_i\rangle\langle\psi_i|) = \mathrm{Tr}(M_m^\dagger M_m\rho)$$

After the measurement of the state described by the initial density matrix ρ and receive the m-th result, the density matrix transforms as follow:

$$\rho_m = \sum_i p_i \frac{M_m|\psi_i\rangle\langle\psi_i|M_m^\dagger}{\mathrm{Tr}(M_m^\dagger M_m\rho)} = \frac{M_m\rho M_m^\dagger}{\mathrm{Tr}(M_m^\dagger M_m\rho)}$$

2.4.3 General quantum operations

If we want to include the influence of the environment on the system time evolution we have to introduce the non-unitary evolution [21],[14], which is irreversible. We start from the assumption that the system is complex: we have the basic system S and the environment E. We can assume that the basis system is independent of the environment:

$$\rho'_{SE} = U(\rho_S \otimes |e_0\rangle\langle e_0|)U^\dagger$$

where the $|e_0\rangle$ is the initial environment state.

To extract the evolution of the basic system we have to perform the partial trace on the environment [21]:

$$\begin{aligned}\rho'_S &= \Lambda(\rho_S)\\ &= \mathrm{Tr}_E(\rho'_{SE})\\ &= \sum_i \langle e_i|\rho'_{SE}|e_i\rangle\\ &= \sum_i E_i\rho_S E_i^\dagger\end{aligned}$$

where the $\{|r_i\rangle\}$ is the environment's orthonormal basis and the E_i is the operator acting in the basic system space:

$$E_i = \langle e_i| U |e_0\rangle$$

Such defined quantum operation Λ we call the quantum channel and it is described by the mapping:

$$\rho' = \Lambda(\rho) = \sum_i E_i \rho E_i^\dagger, \ \sum_i E_i^\dagger E_i \leq \mathbb{1} \tag{2.26}$$

The operator E_i is the Kraus operator [16] and the representation of the quantum operations described by Eq. 2.26 we call the Kraus representation.

Kraus operators are not defined unequivocally due to infinity number of possible the environment's orthonormal basis.

To give the physical meaning for the operation Λ Eq. 2.26 it has to meet four conditions [14]:

$$\rho = \rho^\dagger \Rightarrow \Lambda(\rho) = \Lambda^\dagger(\rho) \tag{2.27}$$

$$\mathrm{Tr}(\rho) = 1 \Rightarrow \mathrm{Tr}(\Lambda(\rho)) = 1 \tag{2.28}$$

$$\rho \geqslant 0 \Rightarrow \Lambda(\rho) \geqslant 0 \tag{2.29}$$

$$\mathcal{H}_S \otimes \mathcal{H}_E \ni \geqslant 0 \Rightarrow (\Lambda_S \otimes \mathbb{1}_E)\rho \geqslant 0 \tag{2.30}$$

where Eq. 2.27 is the hermisity conservation condition, Eq. 2.28 is the trace conservation condition, Eq. 2.29 is positive value conservation condition, Eq. 2.30 requires from the Λ to be completely passivity condition. First three conditions guarantee that the operation $\Lambda(\rho)$ transform the density matrix ρ to the the density matrix ρ'. Additionally, all four conditions are met if and only if $\Lambda(\rho) = \sum_i E_i \rho E_i^\dagger$ for some set of the Kraus operators.

2.5 Compton scattering

The Compton effect is an inelastic scattering process in which a photon scatters on a charged particle (typically electron) [2]. When photon is scattered off, part of its energy is transferred to the electron which causes the reduction of photon frequency [7].

We remind the derivation of the frequency shift equation, first presented by Compton [23]. Let's consider the system presented in the Fig. 2.3, where the incoming photon has the energy $E_i = h\nu$ (frequency ν) and the momentum $\vec{k_i} = \frac{E_i}{c}\hat{k}_i$ (where $\hat{k}_i$ is photon propagation direction), and outgoing photon with the energy $E' = h\nu'$ and momentum $\vec{k'} = \frac{E'}{c}\hat{k}'$. Before the scattering, the electron is at the rest , and it acquires the momentum $\vec{p}$ after the scattering.

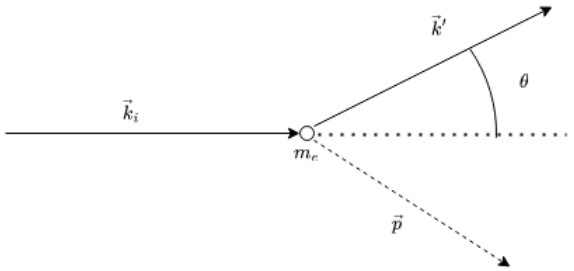

Figure 2.3: System for calculate the frequncy shift.

From the energy and momentum conservation laws we obtain:

$$E_i + m_e c^2 = E' + \sqrt{c^2 p^2 + m_e^2 c^4} \tag{2.31}$$

$$\frac{E_i}{c}\hat{k}_i = \frac{E'}{c}\hat{k}' + \vec{p} \tag{2.32}$$

For the simplicity we can assume that the initial photon propagates along the axis x ($\hat{k}_i = \hat{x}$), then the outgoing photon direction lays on the plane x-y $\hat{k}' = \cos\theta\hat{x} + \sin\theta\hat{y}$, hence, from Eq. 2.32 the electron momentum is:

$$\vec{p} = (p_x, p_y)^T,\ p_x = \frac{E_i}{c} - \frac{E'}{c}\cos\theta,\ p_y = -\frac{E'}{c}\sin\theta$$

and after the substitution of p to Eq. 2.31 we receive the frequency shift:

$$\frac{E'}{E_i} = \frac{\nu'}{\nu} = \frac{1}{1 + \frac{E_i}{\mu}(1 - \cos\theta)},\ \mu = m_e c^2 = 511 \text{ keV} \tag{2.33}$$

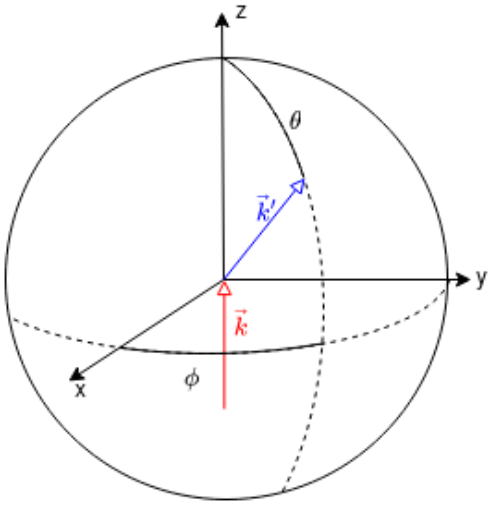

Figure 2.4: Visualization of the Compton scattering. Incoming photon $\vec{k}$ (red arrow) has the same direction as the local z-axis. Outgoing photon $\vec{k}'$ (blue arrow) has a direction defined by the two spherical angles θ, ϕ.

Klein and Nishina derived the cross-section of the polarized scattered photon in the Compton process by solving the perturbed solution of the Dirac equation under the incoming radiation field (photon) [23]. Klein-Nishina formula:

$$\frac{\mathrm{d}\sigma_{pol}}{\mathrm{d}\Omega} = \frac{1}{2}\mathrm{r}_0^2 \left(\frac{E'}{E_i}\right)^2 \left[\frac{E'}{E_i} + \frac{E_i}{E'} - 2(\hat{k}' \cdot \vec{e}_i)\right]$$

where the $\vec{e}_i$ ($\vec{e}_i \cdot \hat{k}_i = 0$) is the incident electric field direction and $\mathrm{r}_0 = \frac{1}{4\pi\varepsilon_0}\frac{e^2}{m_e c^2}$ is the classical electron radius (e is the elementary charge, ε_0 is the vacuum permittivity). We receive more useful form of this equation if we note that the scattering angle (angle between the incident and scattered photon) as $\theta \in [0, \pi]$ and the angle between the scattering direction $\hat{k}'$ and the direction of the polarization $\hat{\epsilon}_i$ of the incident photon as $\phi \in [0, 2\pi]$, which leads to a formula for linearly polarized photons:

$$\frac{\mathrm{d}\sigma_{pol}}{\mathrm{d}\Omega} = \frac{1}{2}\mathrm{r}_0^2 \left(\frac{E'}{E_i}\right)^2 \left[\frac{E'}{E_i} + \frac{E_i}{E'} - 2\sin^2\theta\cos^2\phi\right] \tag{2.34}$$

The differential cross section for unpolarized photon can be obtained by

averaging over azimuthal angle:

$$\begin{aligned}\frac{\mathrm{d}\sigma_{unpol}}{\mathrm{d}\Omega} &= \frac{1}{2\pi}\int_0^{2\pi}\mathrm{d}\phi\frac{\mathrm{d}\sigma_{pol}}{\mathrm{d}\Omega} \\ &= \frac{1}{2}\mathrm{r}_0^2\left(\frac{E'}{E_i}\right)^2\left[\frac{E'}{E_i}+\frac{E_i}{E'}-\sin^2\theta\right]\end{aligned} \tag{2.35}$$

which in the limit $E' \to E_i$ reduces to the Thomson differential cross section:

$$\frac{\mathrm{d}\sigma_T}{\mathrm{d}\Omega} = \lim_{E'\to E_i}\frac{\mathrm{d}\sigma_{unpol}}{\mathrm{d}\Omega} = \frac{1}{2}\mathrm{r}_0^2(1+\cos^2\theta)$$

In Fig. 2.5 the distributions of the differential Compton cross-section as a function of the scattering angle for several incoming photon energies are presented. In Fig. 2.6 the differential cross-sections as a function of scattering polar angle and azimuthal angle, are shown.

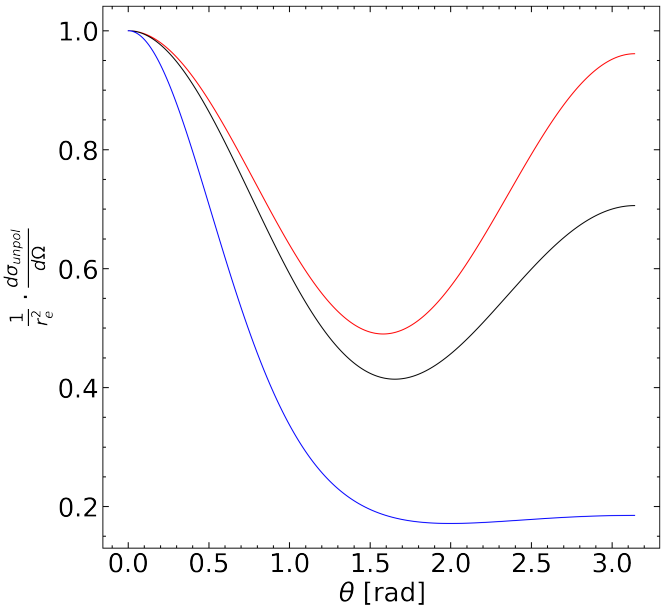

Figure 2.5: The differential cross section Eq. 2.35 for different energies for the incoming photon: $E_i = 0.01\mu$ (red),$E_i = 0.1\mu$ (black),$E_i = 1.0\mu$ (blue). As the photon energy increases, small scattering angles are more preferable.

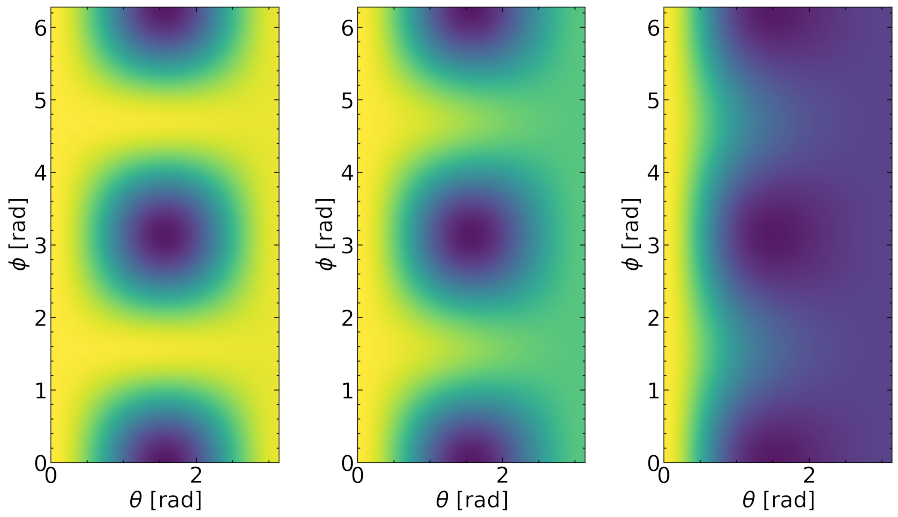

(a) $E_i = 0.01\mu$ (b) $E_i = 0.1\mu$ (c) $E_i = 1.0\mu$

Figure 2.6: The differential cross section Eq. 2.34 for the incoming photon with different energies as a function of the scattering angle θ and azimuthal angle ϕ. The darker the color, the lower the value of the function.

2.6 Compton scattering in the quantum information theory formalism

The Compton scattering of the polarized photon was reformulated in the quantum information formalism in [13]. Here we recall the most important steps of this formulation. We start with the Klein-Nishina formula for the polarized photon as:

$$\frac{\mathrm{d}\sigma_{pol}}{\mathrm{d}\Omega} = \frac{r_0}{2} K^2(k_i,\Theta)\left(\gamma(k_i,\Theta) - 2 + 4|\epsilon_j'^{*}\cdot\epsilon_l|^2\right) \tag{2.36}$$

$$K(k_i,\Theta) = \frac{1}{1+k_i(1-\cos\Theta)} \tag{2.37}$$

$$\gamma(k_i,\Theta) = K(k_i,\Theta) + K^{-1}(k_i,\Theta)$$

$$\cos\Theta = \hat{k_i}\cdot\hat{k'} = \cos\theta'\cos\theta + \cos\big(\phi-\phi'\big)\sin\theta'\sin\theta$$

where the function $K(k_i,\Theta)$ in Eq. 2.37 is redefined the frequency shift Eq. 2.33, ϵ_l is the initial polarization,ϵ_j is the final polarization state, Θ is the scattering angle, $\{\theta,\phi\}$ and $\{\theta',\phi'\}$ are initial $\hat{k}_i$ and final $\hat{k}'$ momentum direction in the spherical coordinates.

We introduce the Kraus operators with respect to the linear polarization basis $\{|H\rangle, |V\rangle\}$ for the initial state with the density matrix ρ[1] where:

$$\mathcal{K}_1 = \sqrt{\gamma(k_i,\Theta) - 2}\mathbb{1}$$

$$\mathcal{K}_2 = \sqrt{2}\begin{pmatrix} f_{HH} & f_{HV} \\ f_{VH} & f_{VV}\end{pmatrix}$$

$$f_{HH} = \big\langle H'\big|H\big\rangle = \cos\theta'\cos\theta\cos\big(\phi-\phi'\big) + \sin\theta'\sin\theta$$

$$f_{HV} = \big\langle H'\big|V\big\rangle = i\cos\theta\sin\big(\phi-\phi'\big)$$

$$f_{VH} = \big\langle V'\big|H\big\rangle = -i\cos\theta'\sin\big(\phi-\phi'\big)$$

$$f_{HV} = \big\langle V'\big|V\big\rangle = \cos\big(\phi-\phi'\big)$$

[1] As pointed in [13] for this Kraus operator definition, the completeness relation:

$$\sum_i \mathcal{K}_i^\dagger\mathcal{K}_i \neq \mathbb{1}$$

is not fulfilled since the term corresponding to energy ratio was factored out.

In the language of Kraus operators the formula Eq. 2.36 transform to:

$$\frac{\mathrm{d}\sigma_{pol}}{\mathrm{d}\Omega} = \frac{r_0}{2} K^2(k_i, \Theta) \sum_{j=1}^{2} \mathrm{Tr}(\mathcal{K}_j \rho \mathcal{K}_j^\dagger) \tag{2.38}$$

This cross-section Eq. 2.38 can be easily generalized to any number n of photons :

$$\frac{\mathrm{d}\sigma_{npol}}{\mathrm{d}\Omega} = \left(\frac{r_0}{2}\right)^n \left(\prod_{k=1}^{n} K^2(k_{i_k}, \Theta_k)\right) \sum_{l_1,\ldots,l_n=1}^{2} \mathrm{Tr}(\mathcal{K}_{l_1}^{(1)} \otimes \ldots \otimes \mathcal{K}_{l_n}^{(n)} \rho \mathcal{K}_{l_1}^{(1)^\dagger} \otimes \ldots \otimes \mathcal{K}_{l_n}^{(n)^\dagger})$$

where $\mathcal{K}_{l_k}^{(k)}$ means l_k-th Kraus operator for the k-th photon (k-th subsystem).

In our studies we focus on the two-photons system:

$$\frac{\mathrm{d}\sigma_{2pol}}{\mathrm{d}\Omega} = \left(\frac{r_0}{2}\right)^2 \left(\prod_{k=1}^{2} K^2(k_{i_k}, \Theta_k)\right) \sum_{l_1,l_2=1}^{2} \mathrm{Tr}(\mathcal{K}_{l_1}^{(1)} \otimes \mathcal{K}_{l_2}^{(2)} \rho \mathcal{K}_{l_1}^{(1)^\dagger} \otimes \mathcal{K}_{l_2}^{(2)^\dagger}) \tag{2.39}$$

Here, we can perform a simple calculations and see one interesting thing which is the independence of the differential cross-sections for the separated state. We start from the two-photons separated state described by the density matrix $\rho_{ab} = \rho_a \otimes \rho_b$ and what we want to see is the fact that the product of two differential cross-sections (each given by the Eq. 2.38) gives us the formula Eq. 2.39 for the matrix ρ_{ab}. To do that we need two properties of the Kronecker product for matrices A,B,C,D:

$$\mathrm{Tr}(A \otimes B) = \mathrm{Tr}(A)\mathrm{Tr}(B) \tag{2.40}$$

$$(A \otimes B)(C \otimes D) = (AC) \otimes (BD) \tag{2.41}$$

Let's focus on the traces:

$$\begin{aligned}
&\sum_{l_a=1}^{2} \mathrm{Tr}(\mathcal{K}_{l_a}^{(a)} \rho_a \mathcal{K}_{l_a}^{(a)^\dagger}) \sum_{l_b=1}^{2} \mathrm{Tr}(\mathcal{K}_{l_b}^{(b)} \rho_b \mathcal{K}_{l_b}^{(b)^\dagger}) \\
&= \sum_{l_a,l_b=1}^{2} \mathrm{Tr}(\mathcal{K}_{l_a}^{(a)} \rho_a \mathcal{K}_{l_a}^{(a)^\dagger}) \mathrm{Tr}(\mathcal{K}_{l_b}^{(b)} \rho_b \mathcal{K}_{l_b}^{(b)^\dagger}) \\
&= \sum_{l_a,l_b=1}^{2} \mathrm{Tr}([\mathcal{K}_{l_a}^{(a)} \rho_a \mathcal{K}_{l_a}^{(a)^\dagger}] \otimes [\mathcal{K}_{l_b}^{(b)} \rho_b \mathcal{K}_{l_b}^{(b)^\dagger}]) \\
&= \sum_{l_a,l_b=1}^{2} \mathrm{Tr}([\mathcal{K}_{l_a}^{(a)} \otimes \mathcal{K}_{l_b}^{(b)}]([\rho_a \mathcal{K}_{l_a}^{(a)^\dagger}] \otimes [\rho_b \mathcal{K}_{l_b}^{(b)^\dagger}])) \\
&= \sum_{l_a,l_b=1}^{2} \mathrm{Tr}([\mathcal{K}_{l_a}^{(a)} \otimes \mathcal{K}_{l_b}^{(b)}][\rho_a \otimes \rho_b][\mathcal{K}_{l_a}^{(a)^\dagger} \otimes \mathcal{K}_{l_b}^{(b)^\dagger}])
\end{aligned}$$

where the third line is the effect of the property Eq. 2.40 and fourth and fifth line are the effect of using Eq. 2.41. The final result is indeed the Eq. 2.39 for separated state.

Before we go further we introduce two additional functions - the envelope function $\mathcal{F}(k_i, \Theta)$ and the visibility $\mathcal{V}(k_i, \Theta)$:

$$\mathcal{F}(k_i, \Theta) = K^2(k_i, \Theta)\left(\gamma(k_i, \Theta) - \sin^2\theta\right) \tag{2.42}$$

$$\mathcal{V}(k_i, \Theta) = \frac{\sin^2\theta}{\gamma(k_i, \Theta) - \sin^2\theta} \tag{2.43}$$

The envelope function is proportional to the differential cross-section of the unpolarized photon Eq. 2.35 up to the constant r_0 and plays role of the amplitude. The visibility function multiplies the interference terms and describes how much the influence of the photon polarization effect is visible in the differential cross-section. Hence, depends on the scattering angle Θ and the initial energy of the photon k_i the polarization effect is more or less visible - in fact, for the scattering angles $\Theta = \{0, \pi\}$ the differential cross-section gives the same results and the one for the unpolarized photon and for specific angle Θ_0 which is the global maximum of the visibility function the polarization effect is the most visible [13]. As consequence only for non-zero visibility the polarization effects can be experimentally probed. The shape of the visibility function for the 511 keV photon is shown in Fig. 2.7.

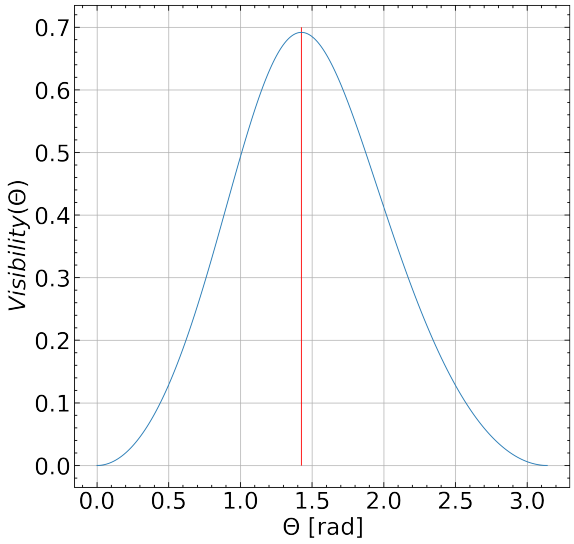

Figure 2.7: The visibility Eq. 2.42 as a function (blue line) of the scattering angle Θ for $k_i = 1$ (511 keV) photon. The red line indicates the position of the function maximum - which is 81.66 deg ($\approx$ 1.4252 rad).

We rewrite Eq. 2.38 in terms of the visibility and the envelope functions:

$$\frac{\mathrm{d}\sigma_{pol}}{\mathrm{d}\Omega} = \frac{r_0}{2}\mathcal{F}(k_i,\Theta)\left(1-\mathcal{V}(k_i,\Theta)\left[(\rho_{HH}-\rho_{VV})\cos(2\Phi)+2Im(\rho_{HV})\sin(2\Phi)\right]\right) \tag{2.44}$$

By using the formula Eq. 2.39 one can calculate the explicit expressions for the differential cross-section depending on the initial state.

2.7 Observables for J-PET experiment

In our studies we consider photon pairs produced from the para-positronium decay [9, 19], which produces two photons each with energy 511 keV ($k_i = 1$). The most favourable condititions for the observation of the photon correlations would correspond to the selection of the scattering region in which the that visibility function is maximized as it was discussed for Eq. 2.44. The maximal visibility is obtained for the the scattering angle of $\Theta_0 = 81.66$ deg.

We will use two kind of histograms: (I) two dimensional histogram which represents a projection of the differential cross-section on the plane $\phi_1 - \phi$ vs $\phi_2 - \phi$. The different interference shapes can be observed for different polarization states. The second histogram (II) is a one-dimensional distribution of $\Delta\phi = \phi_1 - \phi_2$.

We define a weight function $f(x_1, x_2)$ ($x_i = \phi_i - \phi$) for constant scattering angles Θ_1,Θ_2:

$$f(x_1, x_2) = \frac{\frac{\mathrm{d}\sigma_{state}}{\mathrm{d}\Omega}}{\frac{r_0^2}{4}\mathcal{F}(k_i, \Theta_1)\mathcal{F}(k_i, \Theta_2)}$$

mentioned histogram is in this case a sum of above function for different scattering angles. Examples of the theoretical histograms $\phi_a - \phi$ vs $\phi_b - \phi$ for the maximal visibility angle Θ_0 are presented for the separable Fig. 2.8, mixed Fig. 2.9 and entangled Fig. 2.10 states.

To introduce $\Delta\phi$ histogram [9, 19], first we make a variables substitution $\Delta\phi = \phi_1 - \phi_2 = x_1 - x_2$, hence $x_1 = \Delta\phi - x_2$ and to weight function $g(\Delta\phi)$ for such histogram is:

$$g(\Delta\phi) = \frac{\int_{-\phi}^{2\pi-\phi} dx_2 f(\Delta\phi - x_2, x_2)}{\int_{-2\pi}^{2\pi} d\Delta\phi \int_{-\phi}^{2\pi-\phi} dx_2 f(\Delta\phi - x_2, x_2)}$$

where ϕ is the azimuthal angle in the momentum direction vector of the initial photon. Examples of the theoretical $\Delta\phi$ histogram are presented Fig. 2.11 for different polarization states.

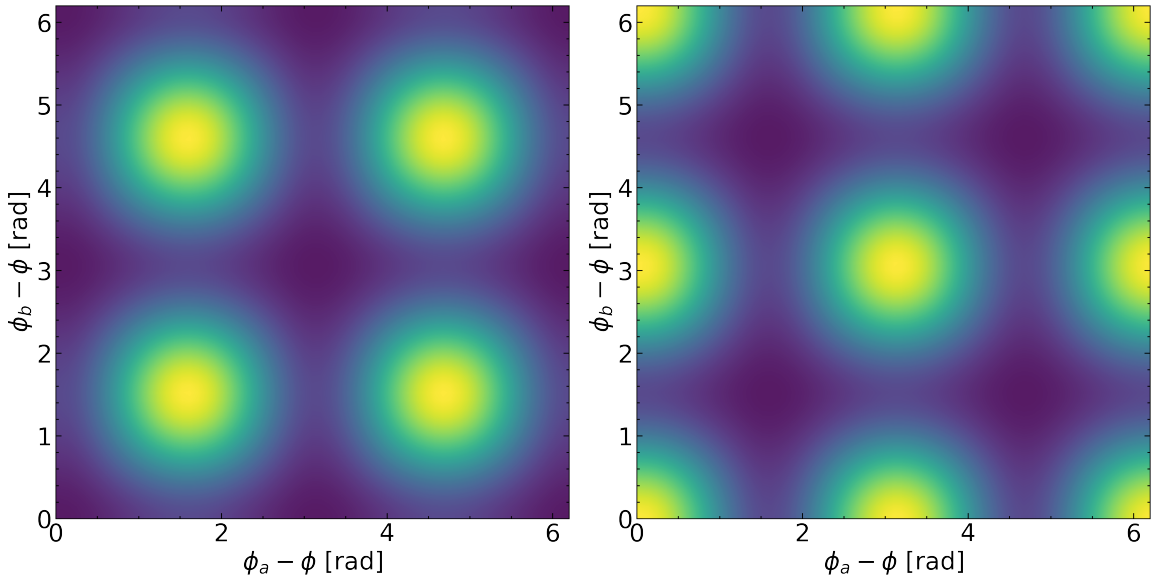

(a) |HH⟩ (b) |VV⟩

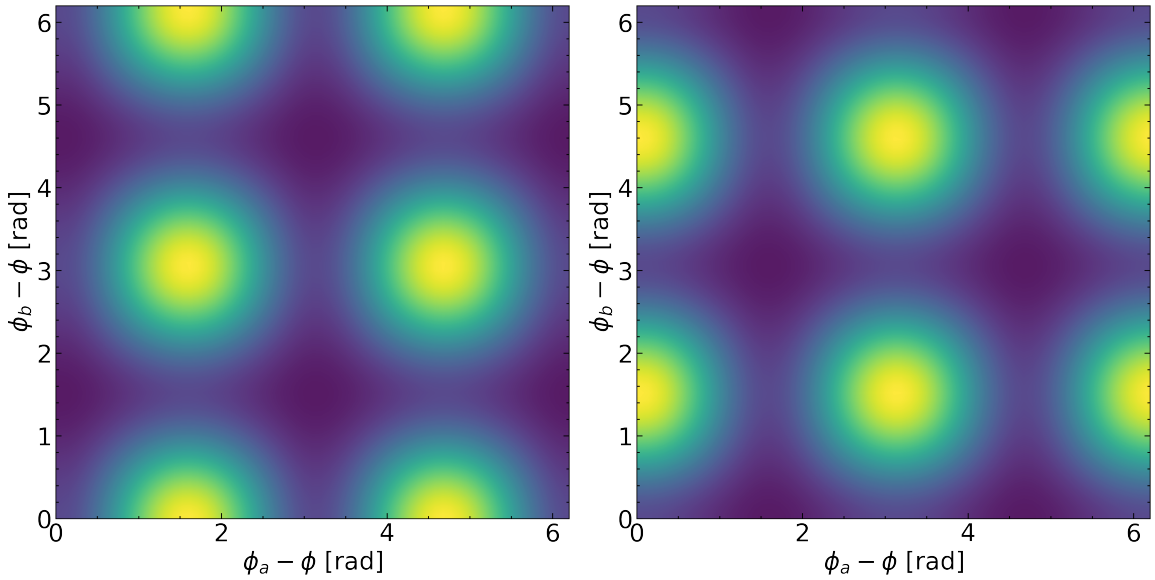

(c) |HV⟩ (d) |VH⟩

Figure 2.8: Histograms $(\phi_b - \phi)$ vs $(\phi_a - \phi)$ ($\Theta_0 = 81.66$ deg) for separable states $|HH\rangle$,$|HV\rangle$,$|VH\rangle$ and $|VV\rangle$. Each state has specific pattern which can be used to distinguish them visually from others.

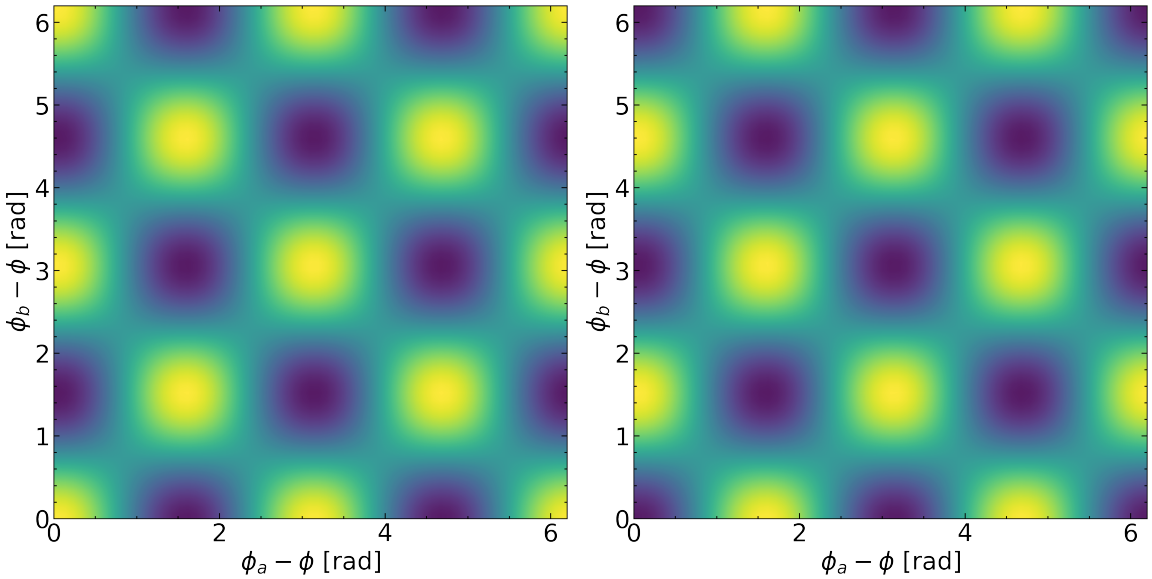

(a) |HH⟩ and |VV⟩ (b) |HV⟩ and |VH⟩

Figure 2.9: Histograms $(\phi_b - \phi)$ vs $(\phi_a - \phi)$ ($\Theta_0 = 81.66$ deg) for the mixed states : $|HH\rangle$ and $|VV\rangle$, $|HV\rangle$ and $|VH\rangle$.

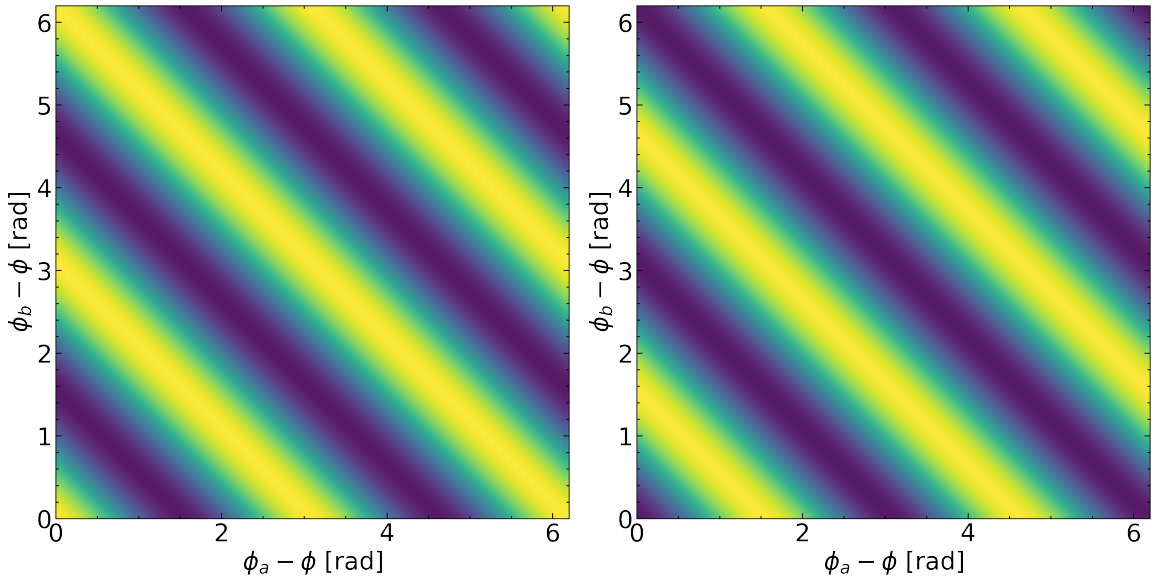

(a) $|\phi^-\rangle$ (b) $|\psi^+\rangle$

Figure 2.10: Histograms $(\phi_b - \phi)$ vs $(\phi_a - \phi)$ ($\Theta_0 = 81.66$ deg) for the entangled states $|\phi^-\rangle = \frac{1}{\sqrt{2}}(|HH\rangle - |VV\rangle)$ and $|\psi^+\rangle = \frac{1}{\sqrt{2}}(|HV\rangle + |VH\rangle)$. The pattern in the histograms is unique for these states and at the same time completely different from those for separable Fig. 2.8 and mixed states Fig. 2.9.

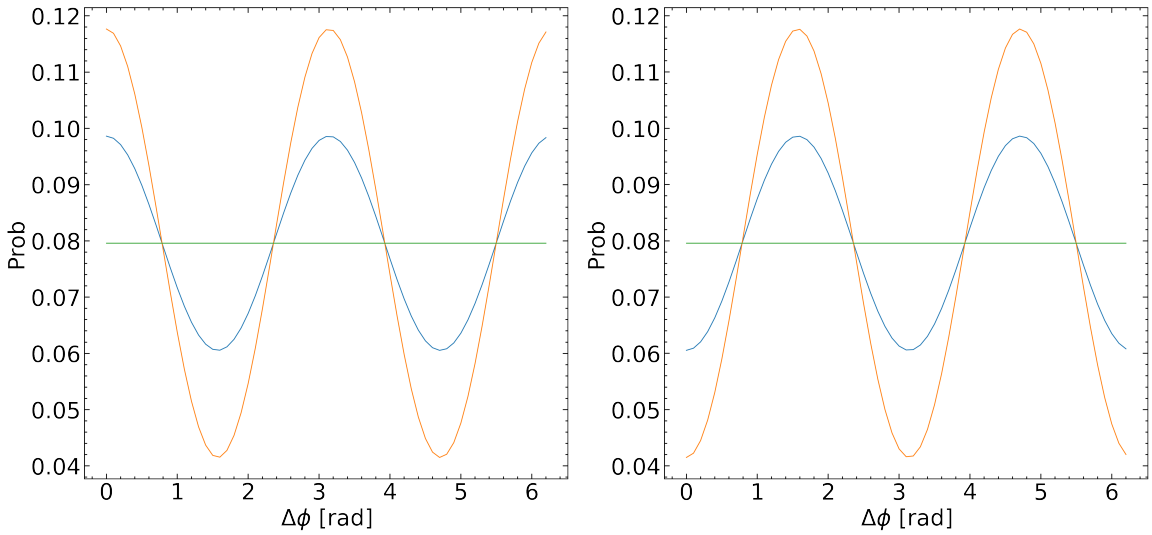

(a) HHVV family (b) HVVH family

Figure 2.11: Comparison of $\Delta\phi$ for different polarization states for the max visibility scattering angle ($\Theta_0 = 81.66$ deg). We can distinguish two groups: (a) HHVV family (states: $|\phi^-\rangle$, $|HH\rangle$,$|VV\rangle$, mix of the $|HH\rangle$ and $|VV\rangle$)); (b) HVVH family (states: $|\psi^-\rangle$, $|HV\rangle$, $|VH\rangle$ and mix of the $|HV\rangle$ and $|VH\rangle$)). In both plots, green line represents unpolarized situation, blue line is a separable (and mixed) state and the orange one is a entangled state. The following conclusions can be drawn from the presented histograms: (1) separable states cannot be distinguished from their statistical mixture; (2) separable states $|HH\rangle$ and $|VV\rangle$ ($|HV\rangle$ and $|VH\rangle$) cannot be distinguished among themselves (to distinguish between them we need $(\phi_b - \phi)$ vs $(\phi_a - \phi)$ histogram); (3) the extremes of the histogram for the entangled state have higher values (up to the absolute value) than for the separable ones.

Chapter 3

Simulation model

We redefine the formula Eq. 2.11 to:

$$|\vec{\epsilon}\rangle_k = \cos\phi_i \, |H\rangle_k + \exp(i\phi_j) \sin\phi_i \, |V\rangle_k$$

where the index $k \in \{a, b\}$ represents the first and second incoming photon, $i \in \{1, 2\}$ is photons index for photons probability amplitude and $j \in 11, 22$ is photons indexes for its global phases. Angle ϕ_i controls polarization's state probability amplitude, ϕ_j controls the global phase value. Vectors $\{|H\rangle_k, |V\rangle_k\}$ construct photon polarization linear basis for given direction of photon (θ_k, ϕ_k). Due to the energy-momentum conservation, the photons originating from the para-positronium decay must propagate in the opposite direction, therefore we can reduce the number of variable into two angles (θ, ϕ) where:

$$\theta_a = \theta, \ \theta_b = \pi - \theta, \ \phi_a = \phi, \ \phi_b = \pi + \phi$$

and polarization states can be described by single basis $\{|H\rangle, |V\rangle\}$ controlled by mentioned two angles as follow:

$$\{|H\rangle_1, |V\rangle_1\} = \{|H\rangle, |V\rangle\}, \{|H\rangle_2, |V\rangle_2\} = \{|H\rangle, -|V\rangle\}$$

which provides general formulas for incoming photons polarization states:

$$|\epsilon\rangle_1 = \cos\phi_1 \, |H\rangle + \exp(i\phi_{11}) \sin\phi_1 \, |V\rangle$$

$$|\epsilon\rangle_2 = \cos\phi_2 \, |H\rangle - \exp(i\phi_{22}) \sin\phi_2 \, |V\rangle$$

Such defined states can be used to declare any separated state for two photons by manipulating four parameters $(\phi_1, \phi_2, \phi_{11}, \phi_{22})$ - examples of values can be found in the Tab. 3.1.

Table 3.1: Examples of $\phi_1, \phi_2, \phi_{11}, \phi_{22}$ parameters values for different separated 2-polarization states in the linear basis $\{|H\rangle, |V\rangle\}$.

State	ϕ_1 [rad]	ϕ_2 [rad]	ϕ_{11} [rad]	ϕ_{22} [rad]
$\|HH\rangle$	0	0	0	0
$\|HV\rangle$	0	$\frac{\pi}{2}$	0	0
$\|VH\rangle$	$\frac{\pi}{2}$	0	0	0
$\|VV\rangle$	$\frac{\pi}{2}$	$\frac{\pi}{2}$	0	0
$\|RL\rangle$	$\frac{\pi}{4}$	$\frac{\pi}{4}$	$\frac{\pi}{2}$	$-\frac{\pi}{2}$

For the separated states we use differential cross-section function as a product of separated photons Eq. 2.36:

$$\frac{\mathrm{d}\sigma_{2pol}}{\mathrm{d}\Omega} = \frac{\mathrm{d}\sigma_{pol}}{\mathrm{d}\Omega}(|\epsilon\rangle_1, |\epsilon'\rangle_1) \cdot \frac{\mathrm{d}\sigma_{pol}}{\mathrm{d}\Omega}(|\epsilon\rangle_2, |\epsilon'\rangle_2) \tag{3.1}$$

To introduce separated and entangled states we have first define the orthogonal polarization states $|\epsilon_\perp\rangle$ such that $\langle\epsilon_\perp|\epsilon\rangle = 0$:

$$|\epsilon_\perp\rangle_1 = -\sin\phi_1 |H\rangle + \exp(i\phi_{11})\cos\phi_1 |V\rangle$$

$$|\epsilon_\perp\rangle_2 = -\sin\phi_2 |H\rangle - \exp(i\phi_{22})\cos\phi_2 |V\rangle$$

and the differential cross-section as:

$$\frac{\mathrm{d}\sigma_{2pol}}{\mathrm{d}\Omega} = \frac{1}{2}\left[\frac{\mathrm{d}\sigma_{pol}}{\mathrm{d}\Omega}(|\epsilon\rangle_1, |\epsilon'\rangle_1) \cdot \frac{\mathrm{d}\sigma_{pol}}{\mathrm{d}\Omega}(|\epsilon\rangle_2, |\epsilon'\rangle_2) + \frac{\mathrm{d}\sigma_{pol}}{\mathrm{d}\Omega}(|\epsilon_\perp\rangle_1, |\epsilon'\rangle_1) \cdot \frac{\mathrm{d}\sigma_{pol}}{\mathrm{d}\Omega}(|\epsilon_\perp\rangle_2, |\epsilon'\rangle_2)\right] \tag{3.2}$$

which realizes the formula Eq. 2.39. Provided formula gives possibility to generated mixed states. To enable entangled states it is required to set additional condition which is:

$$\phi_1 = \phi$$

which is explicitly taking only one slice from the Fig. 2.10. That defined entangled states represents entangled states possible for the para-positronium decay. Such defined states can be used to declare any mixed state and allowed entangled states for two photons by manipulating five parameters $(\phi_1, \phi_2, \phi_{11}, \phi_{22}, \beta)$ - examples of values can be found in the Tab. 3.2.

Table 3.2: Examples of $\phi_1, \phi_2, \phi_{11}, \phi_{22}, \beta$ parameters values for different separated 2-polarization states in the linear basis $\{|H\rangle, |V\rangle\}$.

State	ϕ_1 [rad]	ϕ_2 [rad]	ϕ_{11} [rad]	ϕ_{22} [rad]	β
$\|HH\rangle + \|VV\rangle$	0	0	0	0	False
$\|HV\rangle + \|VH\rangle$	0	$\frac{\pi}{2}$	0	0	False
$\|\psi^+\rangle$	0	$\frac{\pi}{2}$	0	0	True
$\|\phi^-\rangle$	0	$-\pi$	0	0	True

General workflow of the Monte Carlo method can be found on the Fig. 3.1.

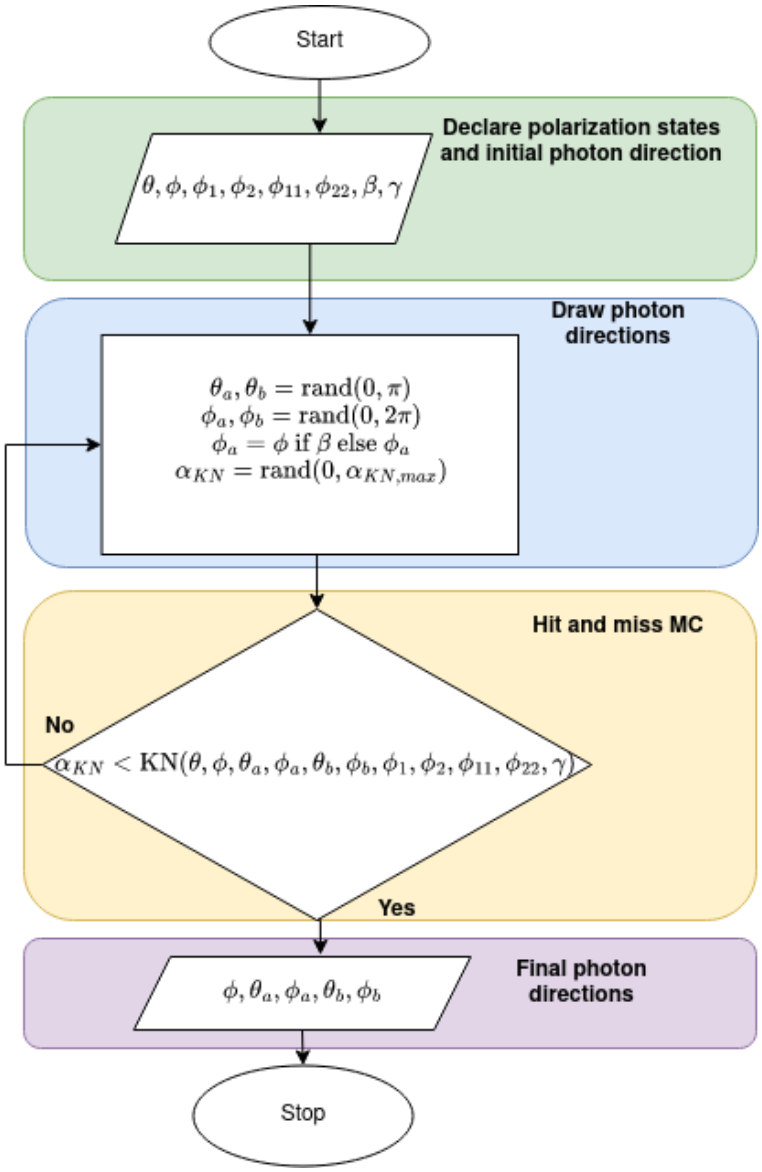

Figure 3.1: Visualization of Monte Carlo method used to simulate Compton scattering for given polarization states $(\phi_1, \phi_2, \phi_{11}, \phi_{22})$ and initial incoming photon direction (θ, ϕ). Drawing of out-coming photons is continued until it meets the Monte Carlo condition. As output are returned directions of first (θ_a, ϕ_a) and second (θ_b, ϕ_b) scattered photon. Parameter β controls simulating of the entangled state. Parameter γ tells which differential cross-section use for the calculations: if γ = False use Eq. 3.1 else use Eq. 3.2. By KN we mean the method which prepares necessary variables and use the proper formula for the differential cross-section calculation.

Another important aspect of the Monte Carlo simulations is to estimate the probing range of the KN function. In the hit and miss method we draw a number from a uniform distribution in a given range $[0, \alpha_{KN,max}]$, where the $\alpha_{KN,max}$ should be greater then maximal value of KN function. This value can be calculated explicitly from the differential cross section, however the faster method is to estimate this number from histogram of KN function values Fig. 3.2 - in this problem the reasonable acceptable value is equal to $\alpha_{KN,max} = 0.9$ under the assumption that the initial energy of emitted gamma is equal 511 keV.

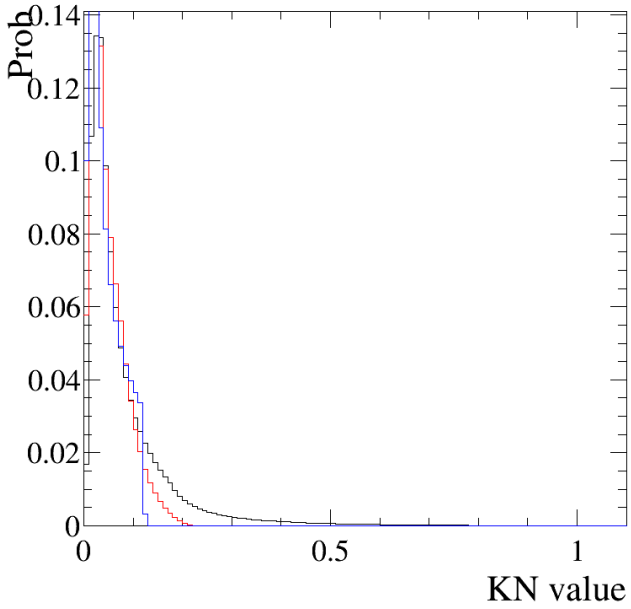

Figure 3.2: Comparison of KN values for different scattering angle ranges for $|HH\rangle$: full range (black), in the circle with radius 30 deg (red) and for a point with max visibility theta (blue). As can be seen from the histogram all values of KN function for different cuts are below values without cuts and maximal value of KN function is lower than 0.8. This histogram was used to estimate the $\alpha_{KN,max} = 0.9$.

Chapter 4

Results

In the experiment , we do not know a priori what is the initial polarization of the photons and what is the fraction of the different polarization states. Furthermore, it must be taken into account that in a real experiment one will be limited by the obtained visibility values.

In the following sub-sections, I present the results of the Monte Carlo simulations for three different categories of polarization states: separable states, mixed states, and entangled states. For each polarization state, I ran three types of simulations:

1. acceptation of all scattering angles Θ_a, Θ_b - this represents situations when we do not impose any selection conditions on the measured data, so the polarization effects should be strongly weakened by the visibility dumping.

2. acceptation of scattering angles Fig. 4.1 limited to the circle $(\Theta_a - \Theta_0)^2 + (\Theta_b - \Theta_0)^2 \leq R_\Theta^2$ ($\Theta_0 = 81.66$ deg, $R_\Theta = 30$ deg) - it represents a situation similar to the real experiment when we measure the scattering angles to a certain extent due to the energy resolution of the detector and the polarization effects should already be significantly visible

3. acceptation of scattering angles equal to the maximum visibility $\Theta_a = \Theta_b = \Theta_0 = 81.66$ deg - this represents an ideal situation in which the effects of photon polarization are revealed in the maximum way.

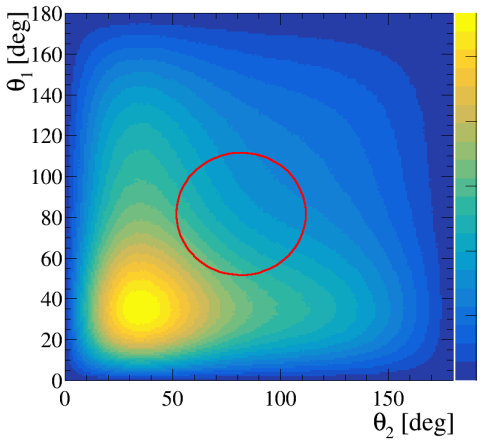

Figure 4.1: Distribution of the scattering angles for the first Θ_a and second Θ_b photon. Red circle (with radius 30 deg around the point $\Theta_a = \Theta_b = \Theta_0 = 81.66$ deg) represents the cut when we accept only scattering angles inside it.

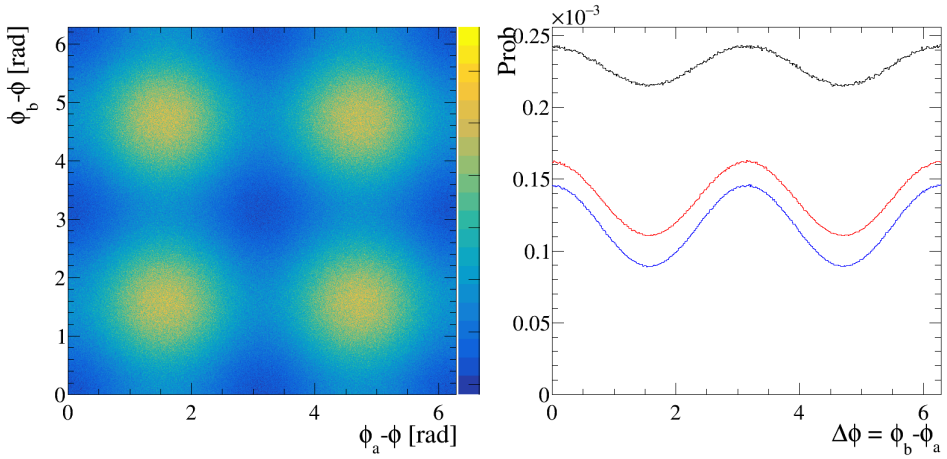

(a) (b)

Figure 4.2: Examples of two types of histograms presented in this section: (a) $\phi_a - \phi$ vs $\phi_b - \phi$ histogram, (b) $\Delta\phi$. Histograms $\Delta\phi$ are always presented as a set of three - each for the different simulation: black line is for all scattering angles, red line is for the scattering angles is the circle and the blue one is for $\Theta_a = \Theta_b = \Theta_0 = 81.66$ deg.

4.1 Separable states

From the separable states I chose four linear polarizations:

$$|\epsilon\rangle = |H\rangle_1 \otimes |H\rangle_2 = |HH\rangle\,,\ \rho_{HH} = \begin{pmatrix} 1 & 0 & 0 & 0 \\ 0 & 0 & 0 & 0 \\ 0 & 0 & 0 & 0 \\ 0 & 0 & 0 & 0 \end{pmatrix}$$

$$|\epsilon\rangle = |H\rangle_1 \otimes |V\rangle_2 = |HV\rangle\,,\ \rho_{HV} = \begin{pmatrix} 0 & 0 & 0 & 0 \\ 0 & 1 & 0 & 0 \\ 0 & 0 & 0 & 0 \\ 0 & 0 & 0 & 0 \end{pmatrix}$$

$$|\epsilon\rangle = |V\rangle_1 \otimes |H\rangle_2 = |VH\rangle\,,\ \rho_{VH} = \begin{pmatrix} 0 & 0 & 0 & 0 \\ 0 & 0 & 0 & 0 \\ 0 & 0 & 1 & 0 \\ 0 & 0 & 0 & 0 \end{pmatrix}$$

$$|\epsilon\rangle = |V\rangle_1 \otimes |V\rangle_2 = |VV\rangle\,,\ \rho_{VV} = \begin{pmatrix} 0 & 0 & 0 & 0 \\ 0 & 0 & 0 & 0 \\ 0 & 0 & 0 & 0 \\ 0 & 0 & 0 & 1 \end{pmatrix}$$

As can be seen each state has its own unique distribution of maxima - explicitly by looking on the histogram we can guess which histogram represents which state and the same situation we have for the shifted histogram Fig. 4.3 - where again we have set of some unique maxima. Even for the full range of scattering angles we have visible similar shape as it was presented in Fig. 2.8, which gains its full shape when we accept only scattering angles equal Θ_0 Fig. 4.5. As can be seen, when we compare results for ideal situation Fig. 4.5 with more realistic model Fig. 4.4 there is no significant differences, which tells us we should observe such polarizations states easily on the histogram if they are present in reality.

From the other side, as it was explained in the section Sec.2.7 we see (Fig. 4.6) that from the histogram $\Delta\phi$ we cannot distinguish between states $(|HH\rangle, |VV\rangle)$ and $(|HV\rangle, |VH\rangle)$ - because of that it is important to plot two dimensional histograms too. Moreover, from the comparison curves i.e. from the Fig. 4.6a we see a huge impact of the selection method on the $\Delta\phi$ shape.

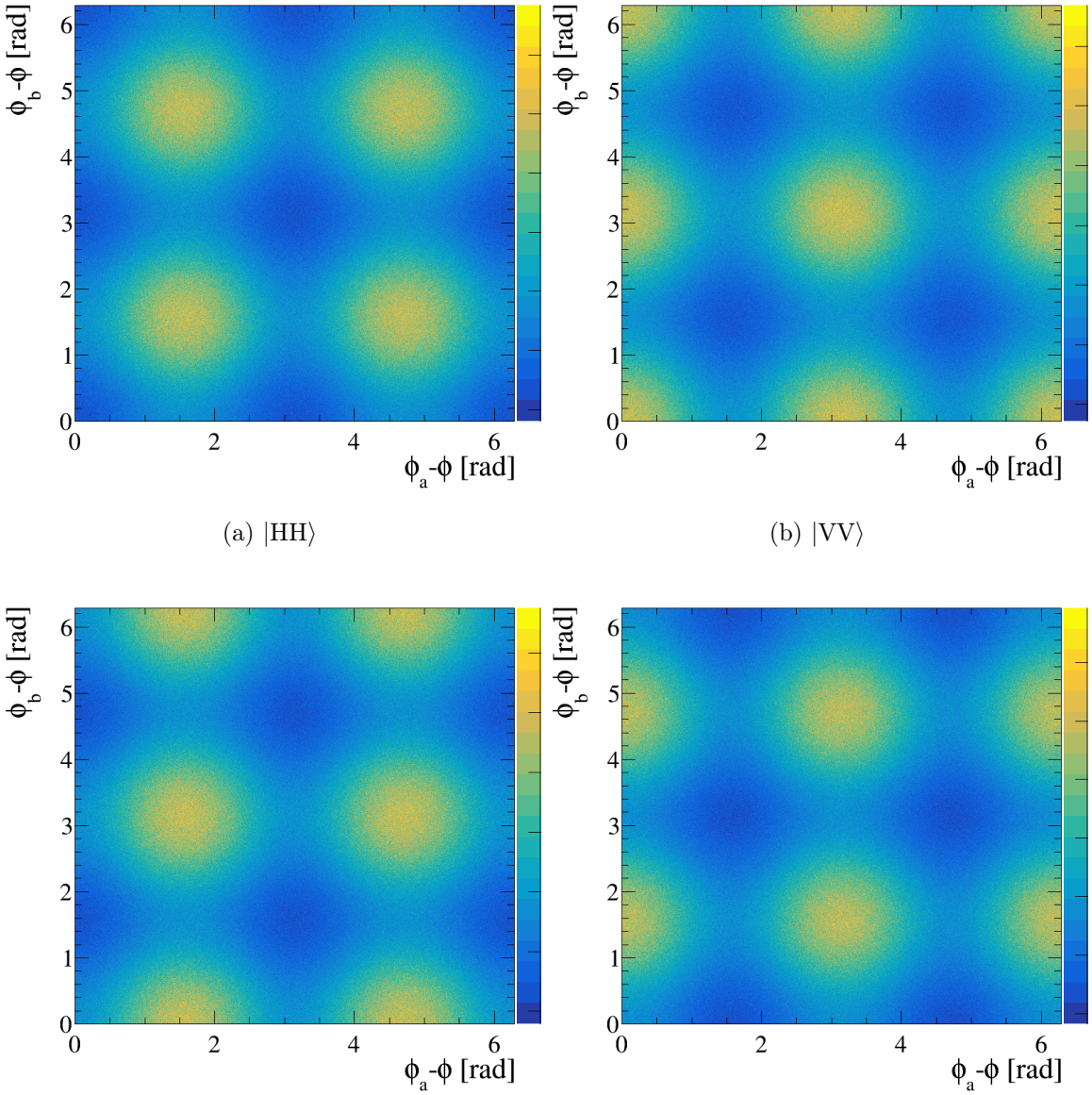

(a) |HH⟩ (b) |VV⟩

(c) |HV⟩ (d) |VH⟩

Figure 4.3: The cross-section projection to the plane $(\phi_b - \phi)$ vs $(\phi_a - \phi)$ for all scattering angles $\theta_1, \theta_2 \in [0, \pi]$ for separable states $|HH\rangle$,$|HV\rangle$,$|VH\rangle$ and $|VV\rangle$.

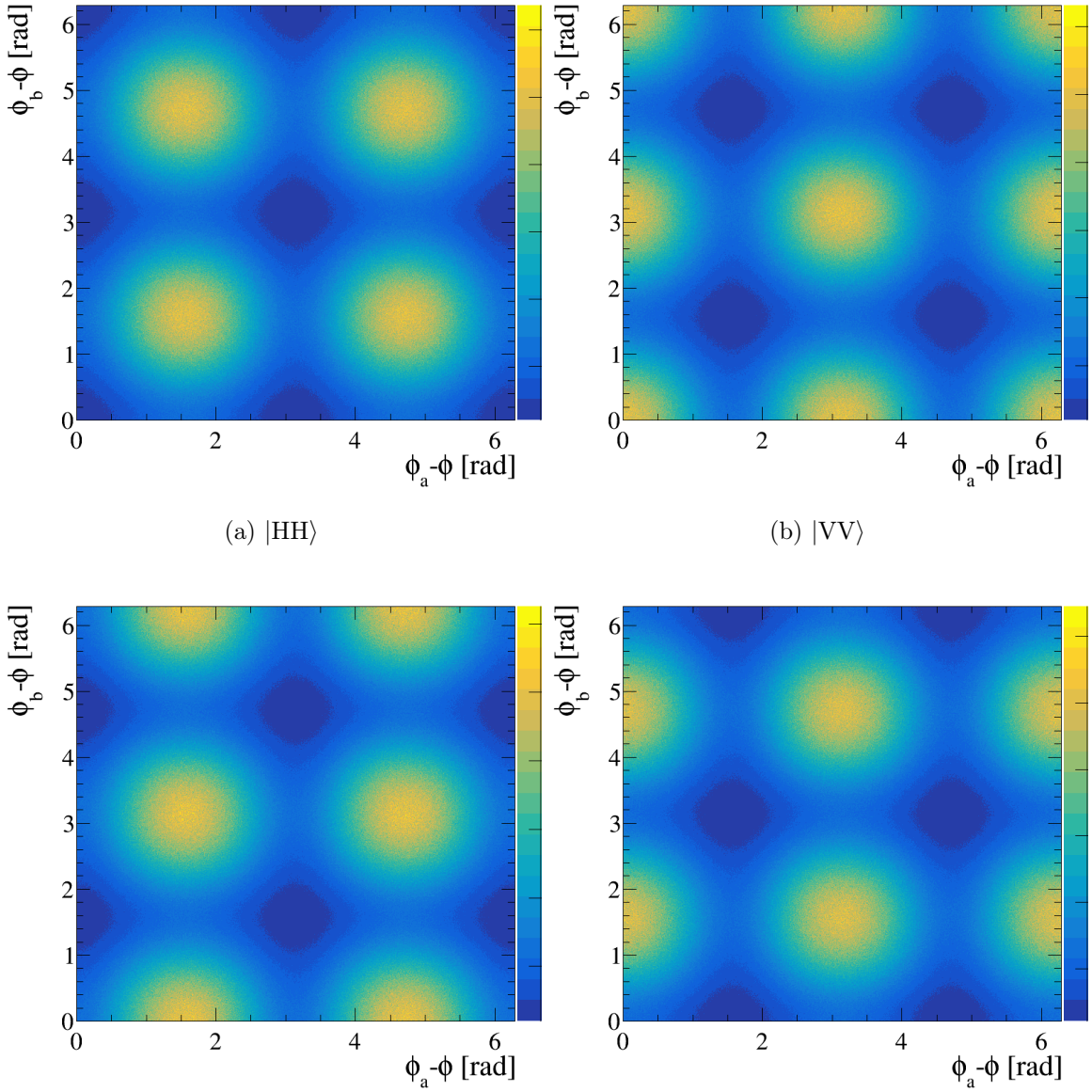

(a) |HH⟩ (b) |VV⟩

(c) |HV⟩ (d) |VH⟩

Figure 4.4: The cross-section projection to the plane $(\phi_b - \phi)$ vs $(\phi_a - \phi)$ for scattering angles in the circle for separable states $|HH\rangle$,$|HV\rangle$,$|VH\rangle$ and $|VV\rangle$.

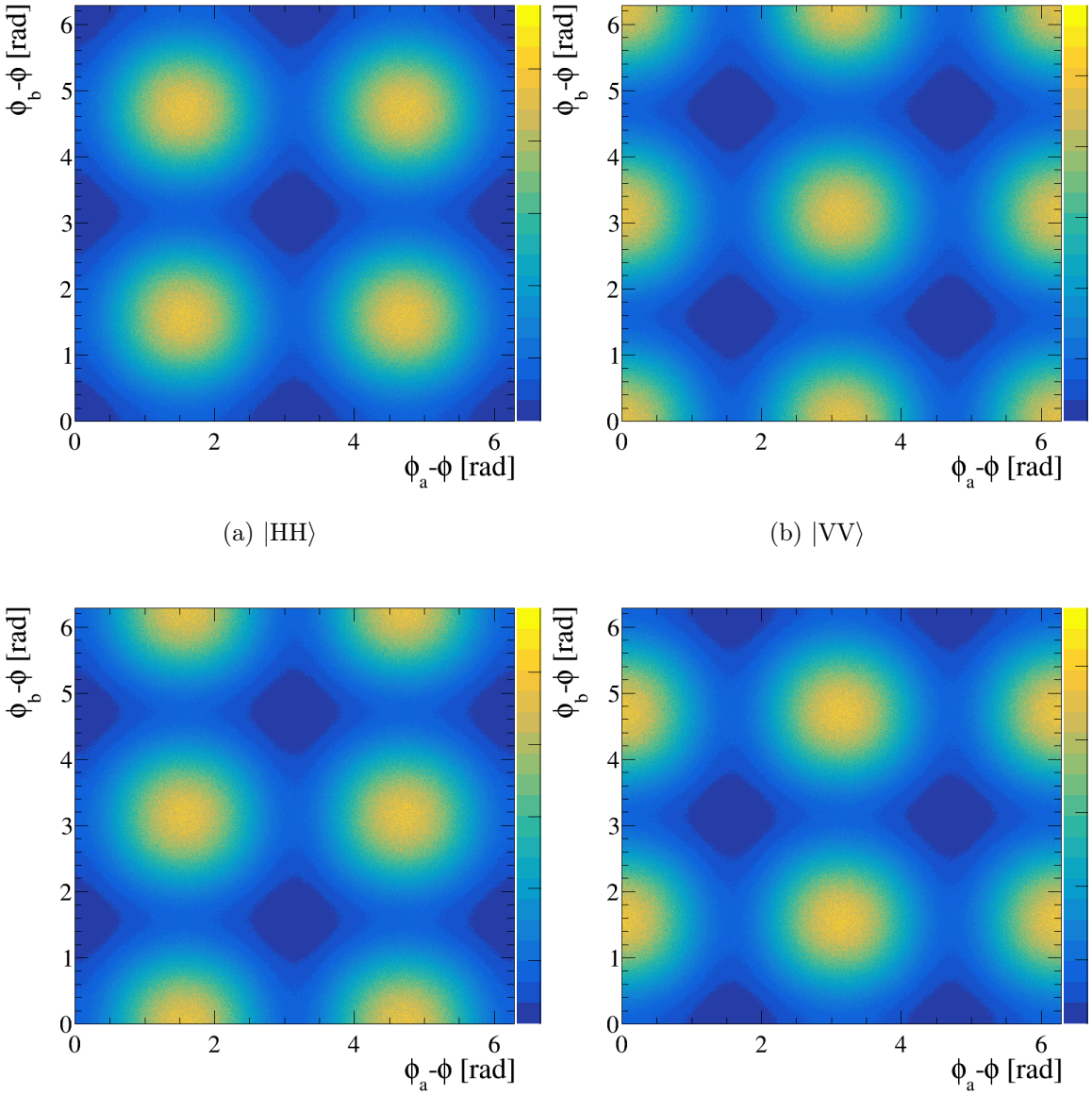

(a) |HH⟩ (b) |VV⟩

(c) |HV⟩ (d) |VH⟩

Figure 4.5: The cross-section projection to the plane $(\phi_b - \phi)$ vs $(\phi_a - \phi)$ for the max visibility scattering angle for separable states $|HH\rangle$,$|HV\rangle$,$|VH\rangle$ and $|VV\rangle$.

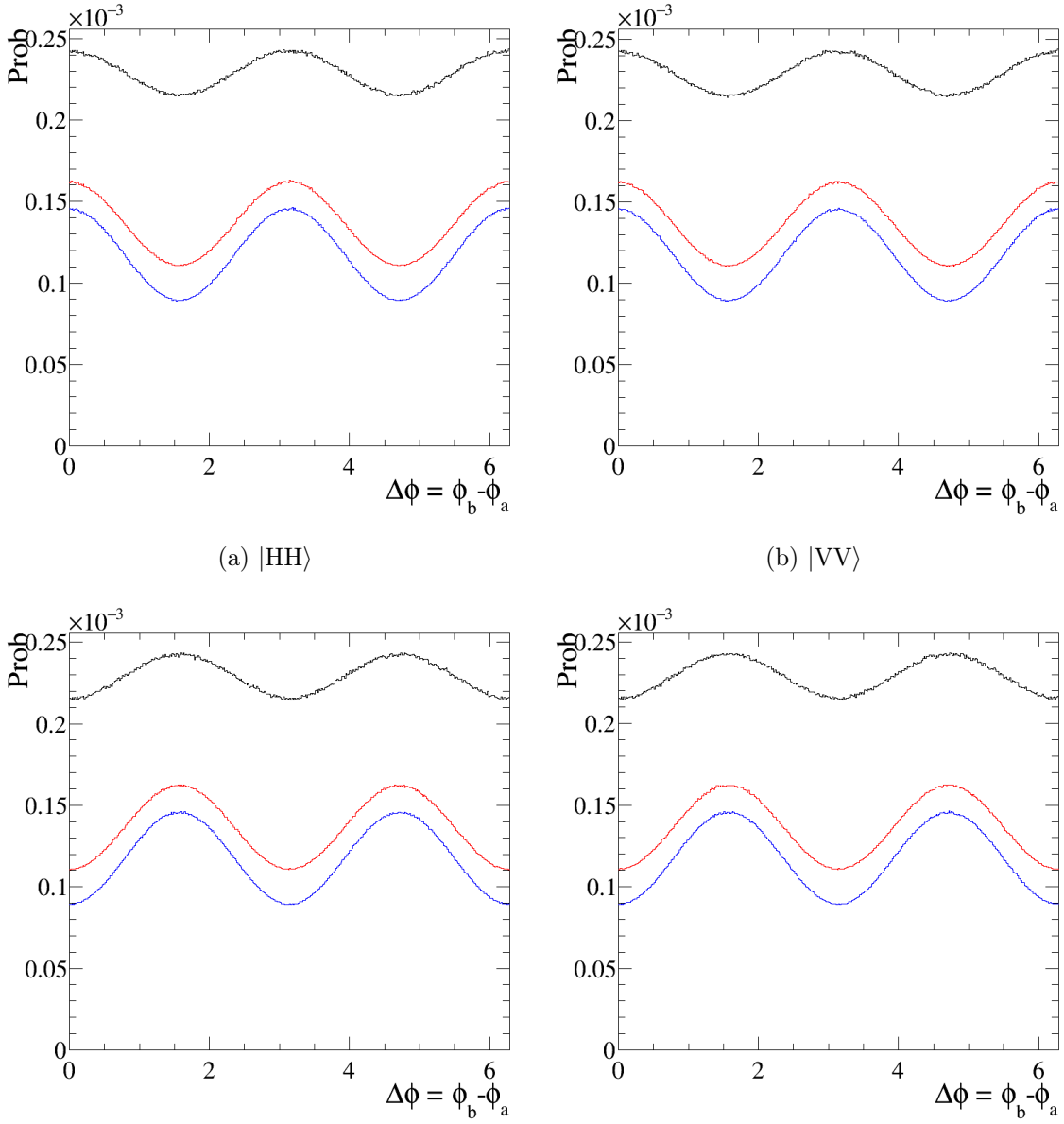

(a) |HH⟩ (b) |VV⟩

(c) |HV⟩ (d) |VH⟩

Figure 4.6: Comparsion of $\Delta\phi$ for different polarization configurations (separable states $|HH\rangle$,$|HV\rangle$,$|VH\rangle$ and $|VV\rangle$) and different selection methods: all scattering angles (black), inside the theta circle (red), max visibility theta (blue).

4.2 Mixed states

As mixed states examples, I chose two linear polarization mixtures :

$$\rho_{HH,VV} = \frac{1}{2}(\rho_{HH} + \rho_{VV}) = \frac{1}{2}\begin{pmatrix} 1 & 0 & 0 & 0 \\ 0 & 0 & 0 & 0 \\ 0 & 0 & 0 & 0 \\ 0 & 0 & 0 & 1 \end{pmatrix}$$

$$\rho_{HV,VH} = \frac{1}{2}(\rho_{HV} + \rho_{VH}) = \frac{1}{2}\begin{pmatrix} 0 & 0 & 0 & 0 \\ 0 & 1 & 0 & 0 \\ 0 & 0 & 1 & 0 \\ 0 & 0 & 0 & 0 \end{pmatrix}$$

However, for the shifted histograms Fig. 4.7 we see something similar to the assembly of the histograms from the Fig. 4.3. We see that with the stricter selection conditions we receive the better image of the situation.

What is the key in this subsection is the observation that from the $\Delta\phi$ histogram we cannot distinguish from it if we have a measurement for the separable state Fig. 4.6 or the mixed state Fig. 4.10 - both histograms have the same shapes and values.

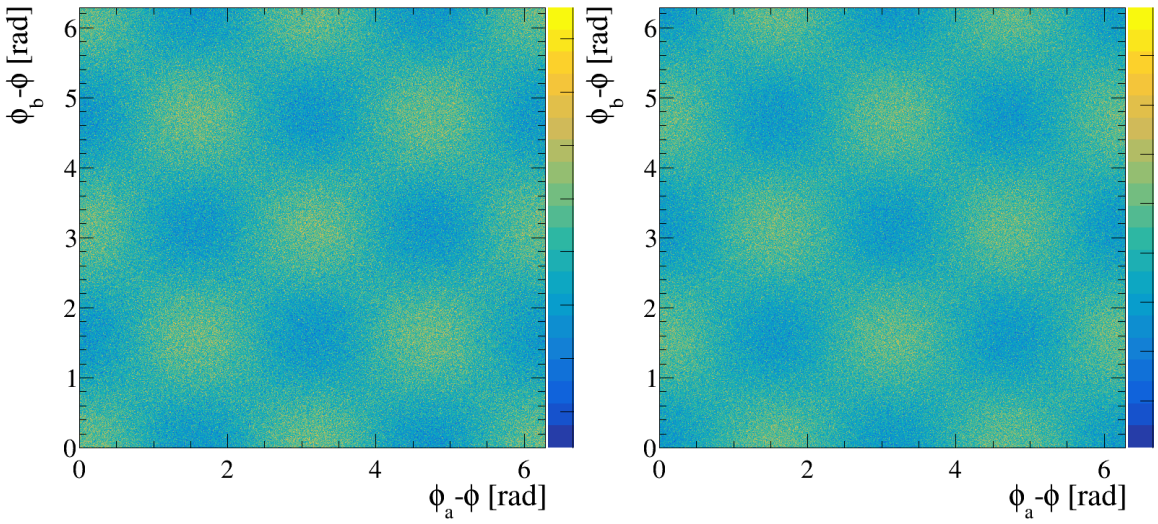

(a) |HH⟩ and |VV⟩ (b) |HV⟩ and |VH⟩

Figure 4.7: The cross-section projection to the plane $(\phi_b - \phi)$ vs $(\phi_a - \phi)$ for all scattering angles $\theta_1, \theta_2 \in [0, \pi]$ for the mixed states : $|HH\rangle$ and $|VV\rangle$, $|HV\rangle$ and $|VH\rangle$.

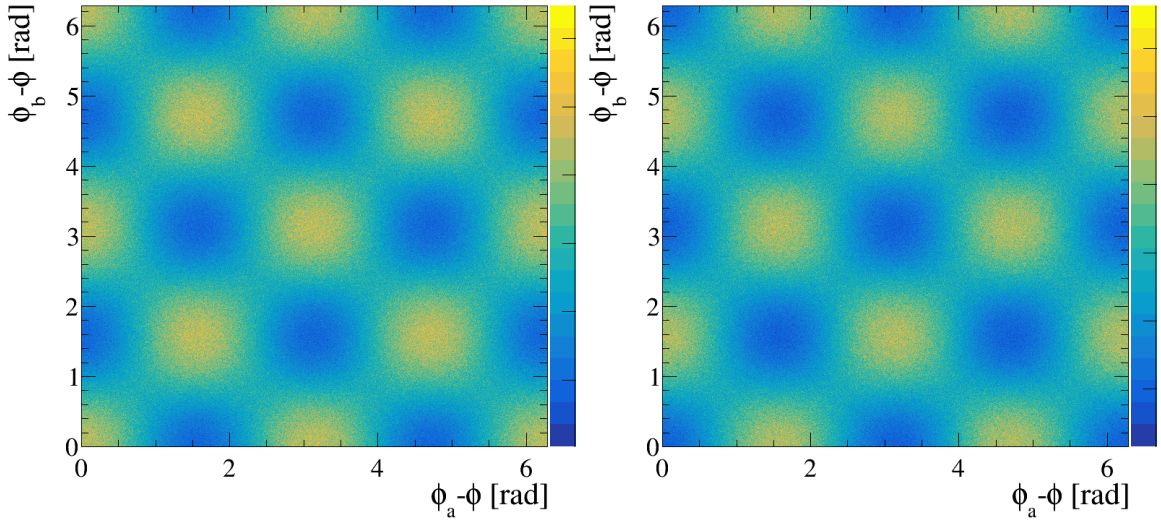

(a) |HH⟩+|VV⟩ (b) |HV⟩+|VH⟩

Figure 4.8: The cross-section projection to the plane $(\phi_b - \phi)$ vs $(\phi_a - \phi)$ for scattering angles in the circle for the mixed states : $|HH\rangle$ and $|VV\rangle$, $|HV\rangle$ and $|VH\rangle$.

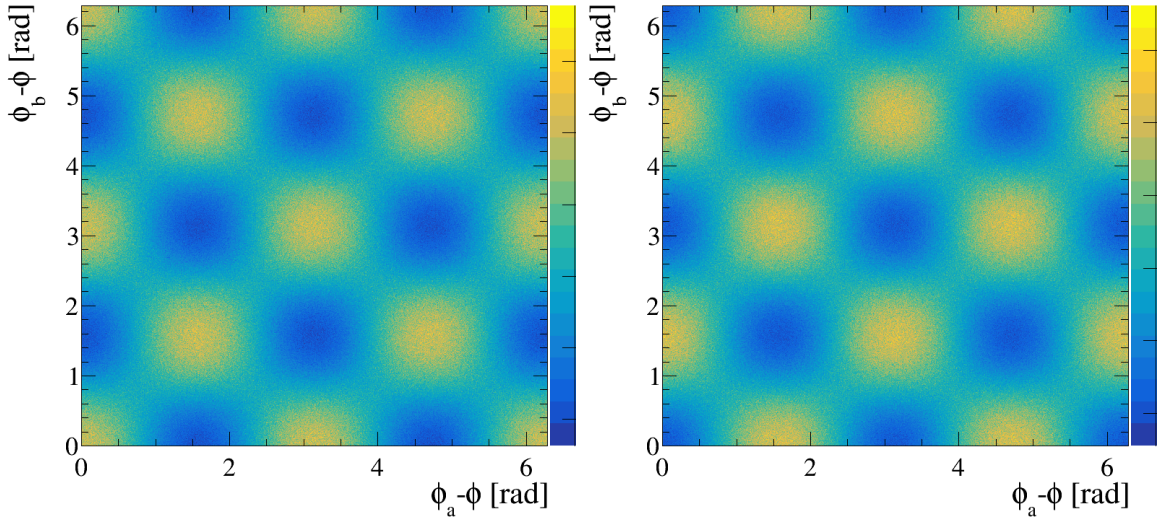

(a) |HH⟩+|VV⟩ (b) |HV⟩+|VH⟩

Figure 4.9: The cross-section projection to the plane $(\phi_b - \phi)$ vs $(\phi_a - \phi)$ for max visibility scattering angle mixed states : $|HH\rangle$ and $|VV\rangle$, $|HV\rangle$ and $|VH\rangle$.

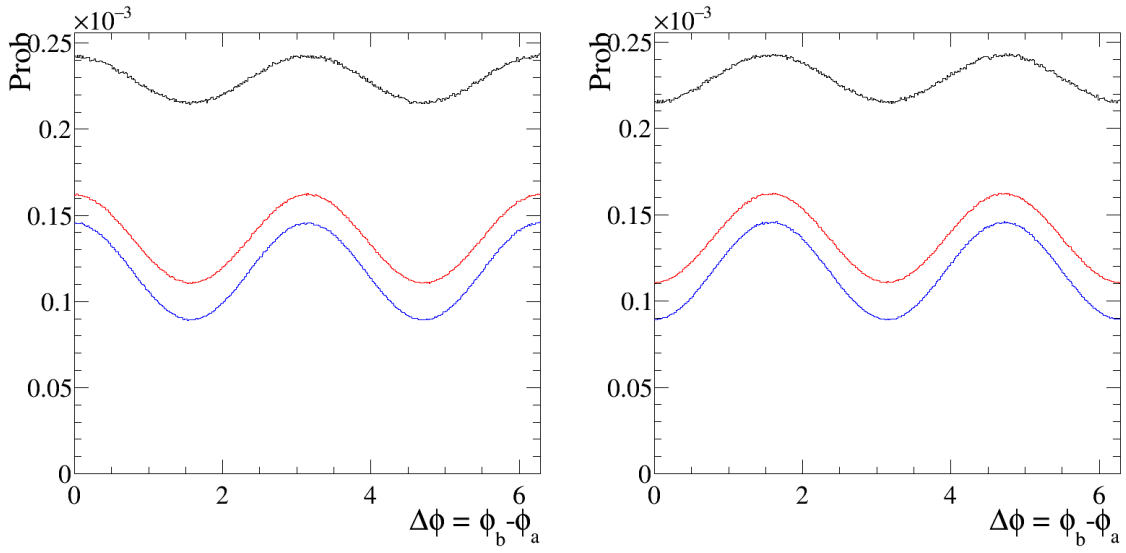

(a) |HH⟩+|VV⟩ (b) |HV⟩+|VH⟩

Figure 4.10: Comparison of $\Delta\phi$ for different polarization configurations (mixed states : $|HH\rangle$ and $|VV\rangle$, $|HV\rangle$ and $|VH\rangle$) and different selection methods: all scattering angles (black), inside the theta circle (red), max visibility theta (blue).

4.3 Entangled states

I chose two entangled states:

$$|\epsilon\rangle = \frac{1}{\sqrt{2}}(|HH\rangle + |VV\rangle) = \left|\phi^-\right\rangle, \ \rho_{\phi^-} = \frac{1}{2}\begin{pmatrix} 1 & 0 & 0 & 1 \\ 0 & 0 & 0 & 0 \\ 0 & 0 & 0 & 0 \\ 1 & 0 & 0 & 1 \end{pmatrix}$$

$$|\epsilon\rangle = \frac{1}{\sqrt{2}}(|HV\rangle + |VH\rangle) = \left|\psi^+\right\rangle, \ \rho_{\psi^+} = \frac{1}{2}\begin{pmatrix} 0 & 0 & 0 & 0 \\ 0 & 1 & 1 & 0 \\ 0 & 1 & 1 & 0 \\ 0 & 0 & 0 & 0 \end{pmatrix}$$

We can say few words about $\Delta\phi$ histogram Fig. 4.11. As can be seen, the stricter selection conditions the more different are histograms of entangled states from the separated states. Generally, we can easily distinguish between separated states $|HH\rangle, |VV\rangle$ and $|\phi^-\rangle$ or $|HV\rangle, |VH\rangle$ and $|\psi^+\rangle$.

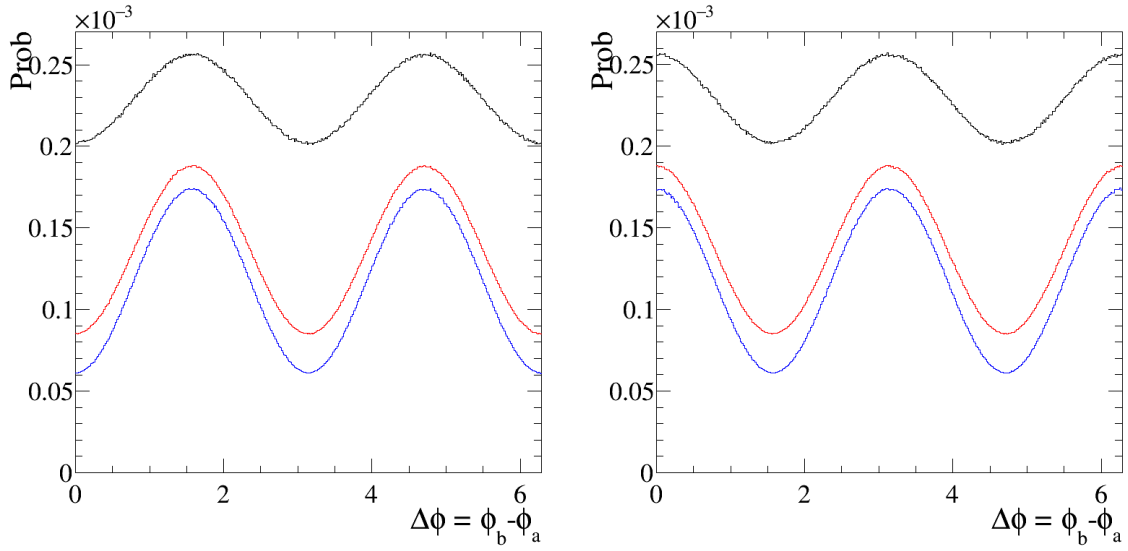

(a) $|\psi^+\rangle$ (b) $|\phi^-\rangle$

Figure 4.11: Comparison of $\Delta\phi$ for different polarization configurations (entangled states: $|\psi^+\rangle$and $|\phi^-\rangle$) and different selection methods: all scattering angles (black), inside the theta circle (red), max visibility theta (blue).

Chapter 5

Summary

In this thesis, the model of a polarized two-photon system probed by the doubly Compton scattering was investigated. The formulation of the Compton process in the quantum information language was used to define the model. Subsequently, the model was implemented in the form of a C++ MC library. The library allows for defining different initial polarization states and includes the visibility effects.

The MC library was used to generate experimental observables such as the difference between the azimuthal angles of the outgoing photons. Different initial polarization states were generated. The interference patterns were compared. The obtained results show that we are able to effectively simulate all the necessary polarization states for a two-photon system from para-positronium decay.

In the next step, the developed model will be incorporated into the Geant4 simulation package. This will enable the simulation of the discussed phenomenon for various detector geometries and the design of an effective selection method for real experimental data gathered by the J-PET collaboration. Finally, different polarization predictions will be compared with the experimental data.

Bibliography

[1] Geant4. https://geant4.web.cern.ch.

[2] *Springer Handbook of Atomic, Molecular, and Optical Physics*. Springer, 2006.

[3] D.R. Bes. *Quantum Mechanics : A Modern and Concise Introductory Course*. Springer, 2007.

[4] G. Chartier. *Introduction to Optics*. Springer, 2005.

[5] M. Chekhova and P. Banzer. *Polarization of light in classical, quantum, and nonlinear optics*. De Gruyter, 2021.

[6] A. S. Chirkin, A. A. Orlov, and D. Y. Parashchuk. Quantum theory of two-mode interactions in optically anisotropic media with cubic nonlinearities: Generation of quadrature and polarization-squeezed light. *Rus. Journ. Quantum Electronics*, 23:870–874, 1993.

[7] D.Greenberger, K.Hentschel, and F.Weinert. *Compendium of Quantum Physics*. Springer, 2009.

[8] J. Dimock. *Quantum Mechanics and Quantum Field Theory*. Cambridge University Press, 2011.

[9] P. Moskal et al. Potential of the j-pet detector for studies of discrete symmetries in decays of positronium atom — a purely leptonic system. *Acta Phys. Pol. B*, 47:509, 2016.

[10] D. Goldstein. *Polarized light*. GRC, 2003.

[11] J. W. Goodman. *Statistical optics*. John Wiley and Sons, 2000.

[12] K.T. Hecht. *Quantum Mechanics*. Springer, 2000.

[13] B. C. Hiesmayr and P. Moskal. Witnessing entanglement in compton scattering processes via mutually unbiased bases. *Scientific Reports*, 9:8166, 2019.

[14] M. Horodecki, P. Horodecki, and R. Horodecki. Mixed state entanglement and quantum communication. in quantum information – an introduction to basic theoretical concepts and experiments. *Springer*, 173:151–195, 2001.

[15] D. Klyshko. *Physical foundations of quantum electronics*. World Scientific, 2011.

[16] K. Kraus. *State, Effects, and Operations*. Springer-Verlag, 1983.

[17] L. Mandel and E. Wolf. *Optical coherence and quantum optics*. Cambridge University Press, 1995.

[18] P. Moskal and A. Gajos et al. Testing cpt symmetry in ortho-positronium decays with positronium annihilation tomography. *Nature Communications*, 12, 2021.

[19] P. Moskal, N. Krawczyk, and B. C. Hiesmayr et al. Feasibility studies of the polarization of photons beyond the optical wavelength regime with the j-pet detector. *Eur. Phys. J. C*, 78:970, 2018.

[20] M.A. Nielsen and I.L. Chuang. *Quantum computation and quantum information*. Cambridge University Press, 2000.

[21] A. Peres. Separability criterion for density matrices. *Phys. Rev. Lett.*, 77:1413–1415, 1996.

[22] W. A. Shurcliff. *Polarized light*. Harward University Press, 1962.

[23] Y. Yazaki. How the klein–nishina formula was derived: Based on the sangokan nishina source materials. *Proc Jpn Acad Ser B Phys Biol Sci.*, 93(6):399–421, 2017.

[24] E. Zeidler. *Quantum Field Theory I: Basics in Mathematics and Physics*. Springer, 2006.